Scottish Universities Environmental Research Centre

Luminescence Dating of Beach Dunes and Fluvial Sediments, Nayarit, Mexico

May 2018

A.J. Cresswell[1], D.C.W. Sanderson[1], E. Muñoz-Salinas[2], M. Castillo[2]

[1]SUERC, East Kilbride, Glasgow
[2]Instituto de Geologia, Universidad Nacional Autónoma de México

East Kilbride Glasgow G75 0QF Telephone: 01355 223332 Fax: 01355 229898

University of Glasgow
The University of Glasgow, charity number SC004401

The University of Edinburgh is a charitable body, registered in Scotland, with registration number SC005336

Summary

The Pacific coast of the state of Nayarit, Mexico, is dominated by extensive sand dune systems and lagoons. 16 samples from three transects through dunes near the town of Santa Cruz were collected to establish ages of the beach dune ridges and establish a robust chronology, to assist in understanding the depositional rates associated with different phases of the evolution of the strand plain. In addition, three samples were collected from a fluvial terrace on the San Pedro River which enters the Pacific near the southernmost of the dune transects. Quartz grains were extracted from the samples, and analysed using an Optically Stimulated Luminescence (OSL) method to determine stored dose and ages.

The samples collected nearest the current coast have produced dates of 1500-1900AD, with samples further from the coast being progressively older, spanning a period of over 2000 years with oldest measured date of 400BC. The dates for the upper samples from the San Pedro River is consistent with the ages of the dunes nearest the coast, with the lower sample date closer to the dates of the older dunes further from the coast, indicating that this fluvial deposit was laid down over the same time period as the dune formation.

Contents

Summary i
1. Introduction 1
2. Methods 3
2.1. Sampling and sample preparation 3
2.1.1. Water contents 4
2.1.2. HRGS and TSBC Sample Preparation 4
2.1.3. Quartz mineral preparation 4
2.2. Measurements and determinations 4
2.2.1. Dose rate determinations 4
2.2.2. Quartz SAR luminescence measurements 5
3. Results 7
3.1. Dose rates 7
3.2. Quartz single aliquot equivalent dose determinations 9
4. Discussion and conclusions 12
References 13
Acknowledgements 13
Appendix A: Dose Response Curves and Probability Distributions 14
Appendix B: Abanico Plots 19

List of figures

Figure 1.1: Location of transects and OSL samples from beach dunes, Nayarit. 1
Figure 1.2: Location of the samples from the San Pedro River. 2
Figure B.1: Abanico Plot for SUTL2941. The dashed line indicates the weighted mean. 19
Figure B.2: Abanico Plot for SUTL2942. The dashed line indicates the weighted mean. 19
Figure B.3: Abanico Plot for SUTL2943. The dashed line indicates the weighted mean. 20
Figure B.4: Abanico Plot for SUTL2944. The dashed line indicates the weighted mean. 20
Figure B.5: Abanico Plot for SUTL2945. The dashed line indicates the weighted mean. 21
Figure B.6: Abanico Plot for SUTL2946. The dashed line indicates the weighted mean. 21
Figure B.7: Abanico Plot for SUTL2947. The dashed line indicates the weighted mean. 22
Figure B.8: Abanico Plot for SUTL2948. The dashed line indicates the weighted mean. 22
Figure B.9: Abanico Plot for SUTL2949. The dashed line indicates the weighted mean. 23
Figure B.10: Abanico Plot for SUTL2950. The dashed line indicates the weighted mean. 23
Figure B.11: Abanico Plot for SUTL2951. The dashed line indicates the weighted mean. 24
Figure B.12: Abanico Plot for SUTL2952. The dashed line indicates the weighted mean. 24
Figure B.13: Abanico Plot for SUTL2953. The dashed line indicates the weighted mean. 25
Figure B.14: Abanico Plot for SUTL2954. The dashed line indicates the weighted mean. 25
Figure B.15: Abanico Plot for SUTL2955. The dashed line indicates the weighted mean. 26
Figure B.16: Abanico Plot for SUTL2956. The dashed line indicates the weighted mean. 26
Figure B.17: Abanico Plot for SUTL2957. The dashed line indicates the weighted mean. 27
Figure B.18: Abanico Plot for SUTL2958. The dashed line indicates the weighted mean. 27

List of tables

Table 2.1: Summary of samples and SUERC laboratory reference codes 3
Table 3.1: Activity and equivalent concentrations of K, U and Th determined by HRGS 7
Table 3.2: Infinite matrix dose rates determined by HRGS and TSBC 8
Table 3.3: Effective beta and gamma dose rates following water correction. It was noted that SUTL2942-2948 were saturated at time of sampling. 9
Table 3.4: SAR quality parameters 10
Table 3.5: Comments on equivalent dose distributions; preferred estimates in bold .. 11
Table 3.6: Quartz OSL ages 12

1. Introduction

The Pacific coast of the state of Nayarit, Mexico, includes an extensive strand plain dominated by sand dune system and lagoons. To assist in understanding the depositional rates associated with different phases of the evolution of the strand plain, samples from transects through dunes near the town of Santa Cruz in the northern part of the state, approximately 90 km north west of the state capital, Tepic, were collected to establish ages of the beach dune ridges and establish a robust chronology of the strand plain. In addition, two samples were collected from a fluvial terrace on the San Pedro River which enters the Pacific near the southernmost of the dune transects.

Three transects were sampled, as illustrated in Fig 1.1. Transect A, at Santa Cruz, is approximately 14 km long with 8 samples taken. Transect B, at Novillero, approximately 45 km to the north of Transect A, is approximately 7 km long with 3 samples taken. Transect C, at Toro Mocho, approximately 30 km to the south of Transect A, is approximately 8 km long with 5 samples taken.

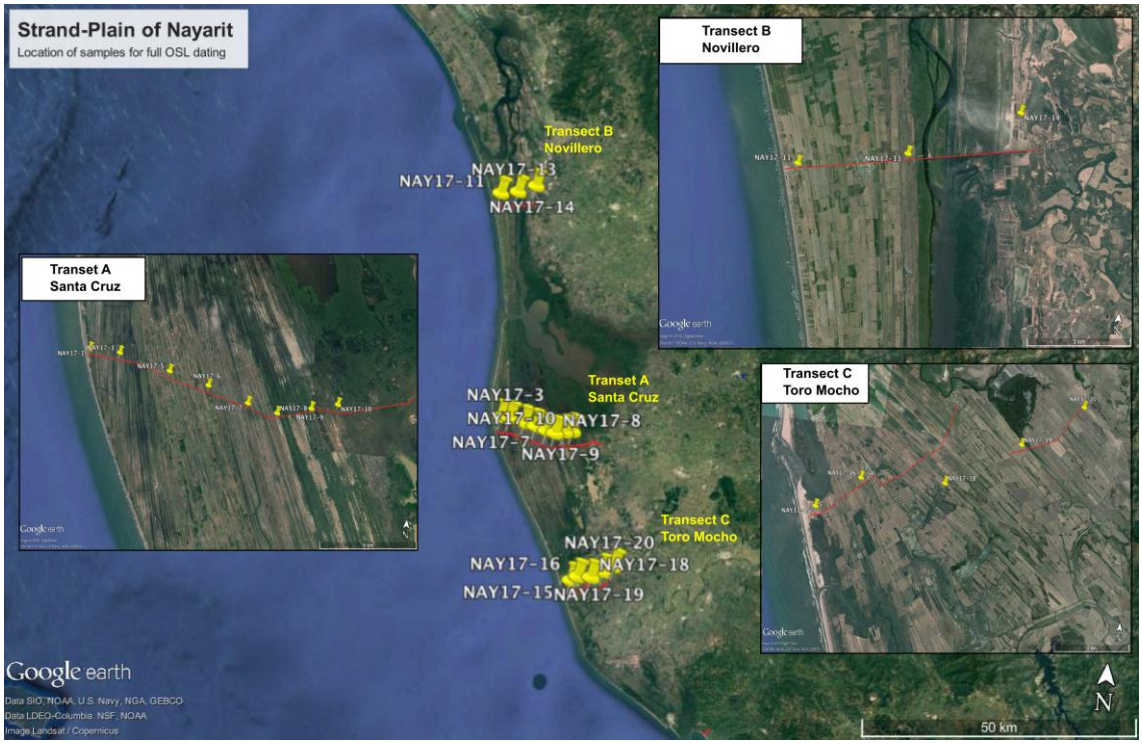

Figure 1.1: Location of transects and OSL samples from beach dunes, Nayarit.

The fluvial samples from the San Pedro River (Fig 1.2) were collected from a site approximately 45 km from the coast, approximately in line with a continuation of Transect A. A profile in a sediment outcrop of a fluvial terrace approximately 10 m from the active channel of the San Pedro River was cut, with samples collected at 100 cm and 200 cm below the surface of the terrace. A third sample at 150cm below the surface of the terrace was supplied after the analysis of the initial two samples.

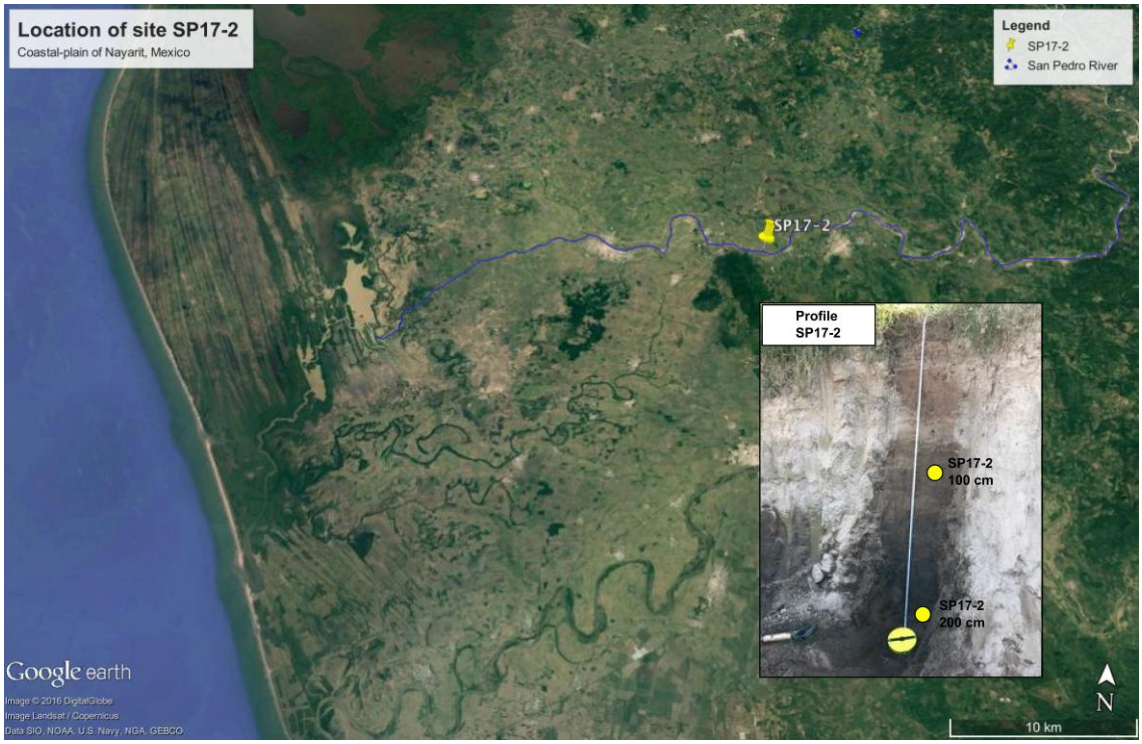

Figure 1.2: Location of the samples from the San Pedro River.

2. Methods

2.1. Sampling and sample preparation

Samples were collected by Esperanza Muñoz-Salinas and colleagues using polyethylene tubes (3 cm diameter, 10 cm long), with at least 500 g of material collected for each sample. The tubes were wrapped in aluminium foil to prevent light exposure during shipment. Additional bulk samples of material were bagged from the same locations for dose rate determination. The dose rate was not measured in the field. Each sample was given a laboratory (SUTL) reference code upon receipt at SUERC, as summarised in Table 2.1.

SUERC code	Description
SUTL2941	Western end of Transect A (Santa Cruz) Beach dune ridge Site code: NAY17-1. Sample extracted at 47 cm depth
SUTL2942	Transect A (Santa Cruz) Beach dune ridge Site code: NAY17-3. Sample extracted at 40 cm depth
SUTL2943	Transect A (Santa Cruz) Beach dune ridge Site code: NAY17-5. Sample extracted at 40 cm depth
SUTL2944	Transect A (Santa Cruz) Beach dune ridge Site code: NAY17-6. Sample extracted at 40 cm depth
SUTL2945	Transect A (Santa Cruz) Beach dune ridge Site code: NAY17-7. Sample extracted at 40 cm depth
SUTL2946	Transect A (Santa Cruz) Beach dune ridge Site code: NAY17-8. Sample extracted at 50 cm depth
SUTL2947	Transect A (Santa Cruz) Beach dune ridge Site code: NAY17-9. Sample extracted at 40 cm depth
SUTL2948	Eastern end of Transect A (Santa Cruz) Beach dune ridge Site code: NAY17-10. Sample extracted at 50 cm depth
SUTL2949	Western end of Transect B (Novillero) Beach dune ridge Site code: NAY17-11. Sample extracted at 80 cm depth
SUTL2950	Transect B (Novillero) Beach dune ridge Site code: NAY17-13. Sample extracted at 60 cm depth
SUTL2951	Eastern end of Transect B (Novillero) Beach dune ridge Site code: NAY17-14. Sample extracted at 60 cm depth
SUTL2952	Western end of Transect C (Toro Mocho) Beach dune ridge Site code: NAY17-15. Sample extracted at 100 cm depth
SUTL2953	Transect C (Toro Mocho) Beach dune ridge Site code: NAY17-16. Sample extracted at 100 cm depth
SUTL2954	Transect C (Toro Mocho) Beach dune ridge Site code: NAY17-18. Sample extracted at 110 cm depth
SUTL2955	Transect C (Toro Mocho) Beach dune ridge Site code: NAY17-19. Sample extracted at 100 cm depth
SUTL2956	Eastern end of Transect C (Toro Mocho) Beach dune ridge Site code: NAY17-20. Sample extracted at 70 cm depth
SUTL2957	San Pedro, ~10 m from the active channel. Fluvial sediment Site code: SP17-2 100cm. Sample extracted at 100 cm depth
SUTL2958	San Pedro, ~10 m from the active channel. Fluvial sediment Site code: SP17-2 200cm. Sample extracted at 200 cm depth
SUTL2971	San Pedro, ~10 m from the active channel. Fluvial sediment Site code: SP17-2 150cm. Sample extracted at 150 cm depth

Table 2.1: Summary of samples and SUERC laboratory reference codes

It was noted that for SUTL2942-2948 (Transect A, excluding the first sample) the sampling hole filled with water.

2.1.1. Water contents

The tube samples were weighed, saturated with water and re-weighed. Following oven drying at 50°C to constant weight, the actual and saturated water contents were determined as fractions of dry weight. These data were used, together with information on field conditions to determine water contents and an associated water content uncertainty for use in dose rate determination.

2.1.2. HRGS and TSBC Sample Preparation

From each of the tube samples, 20 g of the dried material was used in thick source beta counting (TSBC; Sanderson, 1988). Bulk quantities of material, weighing approximately 200 g, were removed from each full dating and bulk sediment sample for environmental dose rate determinations. These dried materials were transferred to high-density-polyethylene (HDPE) pots and sealed with epoxy resin for high-resolution gamma spectrometry (HRGS). Each pot was stored for 3 weeks prior to measurement to allow equilibration of ^{222}Rn daughters.

2.1.3. Quartz mineral preparation

Approximately 20 g of material was removed for each tube and processed to obtain sand-sized quartz grains for luminescence measurements. Each sample was wet sieved to obtain the 90-150 and 150-250 µm fractions. The 150-250 µm fractions were treated with 1 M hydrochloric acid (HCl) for 10 minutes, 15% hydrofluoric acid (HF) for 15 minutes, and 1 M HCl for a further 10 minutes. The HF-etched sub-samples were then centrifuged in sodium polytungstate solutions of ~2.58, 2.62, and 2.74 g cm^{-3}, to obtain concentrates of potassium-rich feldspars (<2.58 g cm^{-3}), sodium feldspars (2.58-2.62 g cm^{-3}) and quartz plus plagioclase (2.62-2.74 g cm^{-3}). The selected quartz fraction was then subjected to further HF and HCl washes (40% HF for 40 mins, followed by 1M HCl for 10 mins).

All materials were dried at 50°C and transferred to Eppendorf tubes. The 40% HF-etched, 2.62-2.74 g cm^{-3} 'quartz' 150-250 µm fractions were dispensed to 10 mm stainless steel discs for measurement. 16 aliquots were dispensed for each sample. The purity of which was checked using a Hitachi S-3400N scanning electron microscope (SEM), coupled with an Oxfords Instruments INCA EDX system, to determine approximate elemental concentrations for each sample.

2.2. Measurements and determinations

2.2.1. Dose rate determinations

Dose rates were measured in the laboratory using HRGS and TSBC. Full sets of laboratory dose rate determinations were made for all samples.

HRGS measurements were performed using a 50% relative efficiency "n" type hyper-pure Ge detector (EG&G Ortec Gamma-X) operated in a low background lead shield with a copper liner. Gamma ray spectra were recorded over the 30 keV to 3 MeV range from each sample, interleaved with background measurements and measurements from SUERC Shap Granite standard in the same geometries. Sample counts were for 80 ks. The spectra were analysed to determine count rates from the major line emissions from ^{40}K (1461 keV), and from selected nuclides in the U decay series (^{234}Th, ^{226}Ra + ^{235}U, ^{214}Pb, ^{214}Bi and ^{210}Pb) and the Th decay series (^{228}Ac, ^{212}Pb, ^{208}Tl) and their statistical counting uncertainties. Net rates and activity concentrations for each of these nuclides were determined relative to Shap Granite by weighted combination of the individual lines for each nuclide. The internal consistency of nuclide specific estimates for U and Th decay series nuclides was assessed relative to measurement precision, and weighted combinations used to estimate mean activity concentrations (Bq kg^{-1}) and elemental concentrations (% K and ppm U, Th) for the parent activity. These data were used to determine infinite matrix dose rates for alpha, beta and gamma radiation.

Beta dose rates were also measured directly using the SUERC TSBC system (Sanderson, 1988). Count rates were determined with six replicate 600 s counts on each sample, bracketed by background measurements and sensitivity determinations using the Shap Granite secondary reference material. Infinite-matrix dose rates were calculated by scaling the net count rates of samples and reference material to the working beta dose rate of the Shap Granite (6.25 ± 0.03 mGy a^{-1}). The estimated errors combine counting statistics, observed variance and the uncertainty on the reference value.

The dose rate measurements were used in combination with the assumed burial water contents, to determine the overall effective dose rates for age estimation. Cosmic dose rates were evaluated by combining latitude and altitude specific dose rates (0.17 ± 0.01 mGy a^{-1}) for the site with corrections for estimated depth of overburden using the method of Prescott and Hutton (1994).

2.2.2. Quartz SAR luminescence measurements

All measurements were conducted using a Risø DA-15 automatic reader equipped with a ^{90}Sr/^{90}Y β-source for irradiation, blue LEDs emitting around 470 nm and infrared (laser) diodes emitting around 830 nm for optical stimulation, and a U340 detection filter pack to detect in the region 270-380 nm, while cutting out stimulating light (Bøtter-Jensen et al., 2000).

Equivalent dose determinations were made on sets of 16 aliquots per sample, using a single aliquot regeneration (SAR) sequence (cf Murray and Wintle, 2000). Using this procedure, the OSL signal levels from each individual disc were calibrated to provide an absorbed dose estimate (the equivalent dose) using an interpolated dose-response curve, constructed by regenerating OSL signals by beta irradiation in the laboratory. Sensitivity changes which may occur as a result of readout, irradiation and preheating (to remove unstable radiation-induced signals) were monitored using small test doses after each regenerative dose. Each measurement was standardised to the test dose response determined immediately after its readout, to compensate for changes in sensitivity during the laboratory measurement sequence. The regenerative doses were

chosen to encompass the likely value of the equivalent (natural) dose. A repeat dose point was included to check the ability of the SAR procedure to correct for laboratory-induced sensitivity changes (the 'recycling test'), a zero dose point is included late in the sequence to check for thermally induced charge transfer during the irradiation and preheating cycle (the 'zero cycle'), and an IR response check included to assess the magnitude of non-quartz signals. Regenerative dose response curves were constructed using doses of 2.5, 5.0, 10, 20 and 30 Gy, with test doses of 1.0 Gy. The 16 aliquot sets were sub-divided into four subsets of four aliquots, such that four preheating regimes were explored (200°C, 220°C, 240°C and 260°C).

3. Results

3.1. Dose rates

HRGS results are shown in Table 3.1, both as activity concentrations (i.e. disintegrations per second per kilogram) and as equivalent parent element concentrations (in % and ppm), based in the case of U and Th on combining nuclide specific data assuming decay series equilibrium.

SUTL no.		Activity Concentration[a] / Bq kg^{-1}			Equivalent Concentration[b]		
		K	U	Th	K / %	U / ppm	Th / ppm
2941	Tube	592 ± 13	37.0 ± 1.4	27.1 ± 1.0	1.92 ± 0.04	3.00 ± 0.11	6.67 ± 0.24
	Bulk	580 ± 18	33.0 ± 1.8	29.3 ± 1.4	1.88 ± 0.06	2.67 ± 0.14	7.22 ± 0.35
2942	Tube	820 ± 20	23.7 ± 1.6	26.5 ± 1.4	2.65 ± 0.06	1.92 ± 0.13	6.52 ± 0.34
	Bulk	824 ± 21	22.5 ± 1.6	26.4 ± 1.4	2.66 ± 0.07	1.82 ± 0.13	6.51 ± 0.35
2943	Tube	773 ± 18	19.6 ± 1.5	21.3 ± 1.3	2.50 ± 0.06	1.59 ± 0.12	5.26 ± 0.31
	Bulk	777 ± 13	19.7 ± 1.1	21.2 ± 1.0	2.51 ± 0.04	1.59 ± 0.09	5.22 ± 0.24
2944	Tube	739 ± 17	25.2 ± 1.6	26.0 ± 1.2	2.39 ± 0.06	2.04 ± 0.13	6.41 ± 0.31
	Bulk	730 ± 15	29.8 ± 1.3	25.7 ± 1.1	2.36 ± 0.05	2.41 ± 0.11	6.35 ± 0.26
2945	Tube	671 ± 14	24.0 ± 1.2	20.6 ± 1.0	2.17 ± 0.04	1.94 ± 0.10	5.09 ± 0.25
	Bulk	683 ± 14	24.3 ± 1.2	19.1 ± 1.0	2.21 ± 0.05	1.97 ± 0.10	4.71 ± 0.26
2946	Tube	735 ± 20	25.7 ± 1.6	24.5 ± 1.5	2.38 ± 0.06	2.08 ± 0.13	6.03 ± 0.36
	Bulk	760 ± 20	31.4 ± 1.7	27.8 ± 1.4	2.46 ± 0.06	2.54 ± 0.14	6.86 ± 0.35
2947	Tube	648 ± 14	22.4 ± 1.2	22.3 ± 1.0	2.10 ± 0.04	1.81 ± 0.09	5.50 ± 0.24
	Bulk	778 ± 15	27.6 ± 1.2	24.6 ± 1.0	2.52 ± 0.05	2.23 ± 0.10	6.05 ± 0.24
2948	Tube	749 ± 18	28.0 ± 1.6	24.2 ± 1.3	2.42 ± 0.06	2.27 ± 0.13	5.97 ± 0.31
	Bulk	679 ± 16	25.6 ± 1.3	21.1 ± 1.1	2.19 ± 0.05	2.08 ± 0.10	5.20 ± 0.26
2949	Tube	837 ± 15	23.8 ± 1.2	26.8 ± 1.0	2.71 ± 0.05	1.93 ± 0.10	6.62 ± 0.24
	Bulk	834 ± 20	21.5 ± 1.5	24.4 ± 1.4	2.70 ± 0.06	1.74 ± 0.12	6.00 ± 0.35
2950	Tube	737 ± 13	21.2 ± 1.1	20.8 ± 1.0	2.38 ± 0.04	1.72 ± 0.09	5.14 ± 0.24
	Bulk	663 ± 14	17.8 ± 1.2	18.0 ± 1.0	2.14 ± 0.05	1.44 ± 0.09	4.43 ± 0.25
2951	Tube	830 ± 14	27.0 ± 1.2	30.1 ± 1.0	2.68 ± 0.05	2.18 ± 0.10	7.41 ± 0.24
	Bulk	793 ± 15	29.6 ± 1.3	29.2 ± 1.0	2.57 ± 0.05	2.39 ± 0.11	7.21 ± 0.24
2952	Tube	304 ± 12	61.6 ± 2.0	33.9 ± 1.2	0.98 ± 0.04	4.99 ± 0.16	8.35 ± 0.29
	Bulk	385 ± 15	40.1 ± 1.9	26.2 ± 1.4	1.24 ± 0.05	3.25 ± 0.15	6.46 ± 0.36
2953	Tube	830 ± 19	23.4 ± 1.6	26.2 ± 1.3	2.68 ± 0.06	1.90 ± 0.13	6.45 ± 0.32
	Bulk	723 ± 20	24.0 ± 1.6	22.2 ± 1.4	2.34 ± 0.06	1.94 ± 0.13	5.47 ± 0.35
2954	Tube	836 ± 20	26.9 ± 1.6	23.9 ± 1.4	2.70 ± 0.06	2.18 ± 0.13	5.88 ± 0.36
	Bulk	825 ± 15	25.1 ± 1.3	24.4 ± 1.0	2.67 ± 0.05	2.03 ± 0.10	6.02 ± 0.24
2955	Tube	693 ± 17	29.6 ± 1.7	23.8 ± 1.4	2.24 ± 0.06	2.40 ± 0.13	5.86 ± 0.35
	Bulk	635 ± 16	29.9 ± 1.6	20.2 ± 1.4	2.05 ± 0.05	2.42 ± 0.13	4.98 ± 0.33
2956	Tube	683 ± 14	28.8 ± 1.3	30.7 ± 1.0	2.21 ± 0.04	2.33 ± 0.11	7.57 ± 0.26
	Bulk	663 ± 14	30.1 ± 1.3	31.4 ± 1.1	2.14 ± 0.05	2.44 ± 0.11	7.75 ± 0.26
2957	Tube	762 ± 18	36.9 ± 1.8	35.5 ± 1.5	2.46 ± 0.06	2.99 ± 0.14	8.76 ± 0.37
	Bulk	769 ± 18	39.1 ± 1.8	36.5 ± 1.4	2.49 ± 0.06	3.17 ± 0.15	9.01 ± 0.35
2958	Tube	664 ± 14	43.1 ± 1.5	45.7 ± 1.1	2.15 ± 0.04	3.49 ± 0.12	11.26 ± 0.27
	Bulk	644 ± 13	45.5 ± 1.6	44.8 ± 1.1	2.08 ± 0.04	3.68 ± 0.13	11.04 ± 0.27
2971	Bulk	742 ± 11	41.6 ± 1.2	37.5 ± 0.7	2.40 ± 0.04	3.37 ± 0.10	9.25 ± 0.18

Table 3.1: Activity and equivalent concentrations of K, U and Th determined by HRGS

[a]Shap granite reference, working values determined by David Sanderson in 1986, based on HRGS relative to CANMET and NBL standards.

[b]Activity and equivalent concentrations for U, Th and K determined by HRGS (Conversion factors based on NEA (2000) decay constants): 40K: 309.3 Bq kg^{-1} %K^{-1}, 238U: 12.35 Bq kg^{-1} ppmU^{-1}, 232Th: 4.057 Bq kg^{-1} ppm Th^{-1}

Infinite matrix alpha, beta and gamma dose rates from HRGS are listed for all samples in Table 3.2, together with infinite matrix beta dose rates from TSBC and field gamma dose rates from FGS. Beta dose rates from HRGS are typically lower than those determined from TSBC by approximately 20%. Wet gamma dose rates were measured in situ by FGS for each of the dating positions, and are typically lower than the HGRS gamma dose rates after water content corrections.

SUTL no.	HRGS, dry[a] / mGy a^{-1}			TSBC, dry / mGy a^{-1}
	Alpha	Beta	Gamma[b]	
2941	13.26 ± 0.37	2.22 ± 0.04	1.14 ± 0.02	2.99 ± 0.08
2942	10.16 ± 0.44	2.67 ± 0.06	1.19 ± 0.03	3.72 ± 0.09
2943	8.30 ± 0.41	2.46 ± 0.05	1.06 ± 0.02	3.00 ± 0.08
2944	10.40 ± 0.43	2.47 ± 0.05	1.16 ± 0.02	3.21 ± 0.09
2945	9.16 ± 0.32	2.23 ± 0.04	1.00 ± 0.02	2.70 ± 0.08
2946	10.24 ± 0.46	2.45 ± 0.06	1.18 ± 0.03	3.24 ± 0.09
2947	9.09 ± 0.32	2.16 ± 0.04	1.08 ± 0.02	2.82 ± 0.08
2948	10.71 ± 0.44	2.51 ± 0.05	1.09 ± 0.02	3.18 ± 0.15
2949	10.25 ± 0.32	2.72 ± 0.04	1.19 ± 0.02	3.72 ± 0.15
2950	8.58 ± 0.31	2.38 ± 0.04	0.97 ± 0.02	3.06 ± 0.14
2951	11.55 ± 0.33	2.76 ± 0.04	1.27 ± 0.02	3.65 ± 0.07
2952	20.04 ± 0.49	1.78 ± 0.04	1.12 ± 0.03	2.24 ± 0.07
2953	10.04 ± 0.43	2.69 ± 0.06	1.13 ± 0.03	3.37 ± 0.09
2954	10.41 ± 0.45	2.73 ± 0.06	1.19 ± 0.02	3.54 ± 0.09
2955	10.99 ± 0.45	2.38 ± 0.05	1.07 ± 0.03	2.87 ± 0.08
2956	12.07 ± 0.35	2.39 ± 0.04	1.19 ± 0.02	3.02 ± 0.07
2957	14.79 ± 0.49	2.73 ± 0.05	1.41 ± 0.03	3.48 ± 0.10
2958	18.01 ± 0.49	2.61 ± 0.04	1.49 ± 0.02	3.04 ± 0.10
2971	16.20 ± 0.31	2.75 ± 0.03	1.44 ± 0.02	3.39 ± 0.08

Table 3.2: Infinite matrix dose rates determined by HRGS and TSBC
[a]based on dose rate conversion factors in Aikten (1983) and Sanderson (1987)
[b]average of tube and bulk samples

The water content measurements are given in Table 3.3, together with the assumed values for the average water content during burial. Field (ranging from 3 to 26 % of dry weight) and saturated (18 to 38 % of dry weight) water contents were determined from all samples in the laboratory, with working values for each site adopted for effective dose rate evaluation. Effective dose rates to the HF-etched 150-250 μm quartz grains are given in table 3.3 (the mean of the TSBC and HRGS data, accounting for water content and grain size), together with the estimate of the gamma dose rate (HRGS data, accounting for water content).

SUTL	Water contents / %			Effective Dose Rate / mGy a^{-1}		
no.	Field	Sat	Assumed	Beta[a]	Gamma	Total[b]
2941	9	21	15 ± 5	1.87 ± 0.13	0.98 ± 0.05	3.01 ± 0.14
2942	17	22	20 ± 5	2.20 ± 0.14	0.97 ± 0.05	3.35 ± 0.15
2943	17	18	20 ± 5	1.93 ± 0.12	0.86 ± 0.04	2.97 ± 0.13
2944	20	23	20 ± 5	1.98 ± 0.13	0.95 ± 0.05	3.10 ± 0.14
2945	46	47	45 ± 5	1.40 ± 0.08	0.67 ± 0.03	2.24 ± 0.09
2946	16	18	15 ± 5	2.12 ± 0.15	1.01 ± 0.05	3.30 ± 0.15
2947	17	26	20 ± 5	1.84 ± 0.12	0.89 ± 0.04	2.90 ± 0.12
2948	16	18	15 ± 5	2.04 ± 0.17	0.94 ± 0.05	3.14 ± 0.17
2949	2	32	15 ± 5	2.33 ± 0.18	1.02 ± 0.05	3.52 ± 0.18
2950	17	23	20 ± 5	1.84 ± 0.14	0.80 ± 0.04	2.81 ± 0.15
2951	20	25	20 ± 5	2.21 ± 0.13	1.04 ± 0.05	3.42 ± 0.14
2952	3	20	10 ± 5	1.49 ± 0.11	1.01 ± 0.05	2.67 ± 0.12
2953	6	28	10 ± 5	2.28 ± 0.16	1.02 ± 0.05	3.47 ± 0.17
2954	2	26	10 ± 5	2.42 ± 0.16	1.08 ± 0.06	3.67 ± 0.17
2955	18	23	20 ± 5	1.81 ± 0.12	0.88 ± 0.04	2.85 ± 0.13
2956	13	18	15 ± 5	1.98 ± 0.13	1.02 ± 0.05	3.17 ± 0.14
2957	15	25	20 ± 5	2.17 ± 0.14	1.15 ± 0.06	3.49 ± 0.15
2958	27	30	25 ± 5	1.88 ± 0.12	1.17 ± 0.05	3.22 ± 0.13
2971	22	36	28 ± 5	2.05 ± 0.11	1.10 ± 0.05	3.32 ± 0.12

Table 3.3: Effective beta and gamma dose rates following water correction. It was noted that SUTL2942-2948 were saturated at time of sampling.

[a] Effective beta dose rate combining water content corrections with inverse grain size attenuation factors obtained by weighting the 150-250 μm attenuation factors of Mejdahl (1979) for K, U, and Th by the relative beta dose contributions for each source determined by Gamma Spectrometry;
[b] includes a cosmic dose contribution

3.2. Quartz single aliquot equivalent dose determinations

For equivalent dose determination, data from single aliquot regenerative dose measurements were analysed using the Risø TL/OSL Viewer programme to export integrated summary files that were analysed in MS Excel and SigmaPlot. Composite dose response curves were constructed from selected discs and when possible, for each of the preheating groups from each sample, and used to estimate equivalent dose values for each individual disc and their combined sets. Dose response curves (shown in Appendix A) for each of the preheating temperature groups and the combined data were determined using a fit to a saturating exponential function. Probability density functions (PDFs) were generated to describe the dose distributions, and are also shown in Appendix A.

SAR quality parameters are given in Table 3.4. All of these samples are relatively low sensitivity, with less than 3000 c Gy^{-1}, with an increase in sensitivity of 2-20% per cycle. In most cases, they demonstrate negligible IRSL signals, and in all cases <1 count in the zero cycle. Recycling ratios should be unity, and range from 0.85 to 1.28 with an average of 1.02 ± 0.02.

SUTL no.	Mean sensitivity c Gy^{-1}	Sensitivity change / cycle (%)	Recycling ratio	Zero cycle	IRSL (%)
2941	1546 ± 168	12.3 ± 5.4	1.004 ± 0.064	0.67 ± 0.05	1.0 ± 0.4
2942	479 ± 52	6.4 ± 3.5	0.988 ± 0.091	0.62 ± 0.09	1.8 ± 0.8
2943	365 ± 30	1.8 ± 2.3	1.007 ± 0.117	0.62 ± 0.07	18.4 ± 1.9
2944	391 ± 49	9.4 ± 5.0	1.018 ± 0.082	0.44 ± 0.08	11.4 ± 2.8
2945	1102 ± 128	2.6 ± 3.6	1.034 ± 0.070	0.65 ± 0.06	1.5 ± 0.6
2946	1247 ± 185	6.3 ± 5.3	1.027 ± 0.077	0.64 ± 0.06	1.6 ± 0.8
2947	1612 ± 200	9.6 ± 5.3	0.948 ± 0.024	0.60 ± 0.03	-0.5 ± 0.3
2948	2948 ± 259	17.7 ± 4.7	0.868 ± 0.019	0.51 ± 0.03	0.1 ± 0.1
2949	517 ± 54	2.4 ± 3.3	1.100 ± 0.081	0.77 ± 0.08	-1.9 ± 1.5
2950	389 ± 59	3.2 ± 4.8	1.050 ± 0.069	0.65 ± 0.05	5.3 ± 1.1
2951	436 ± 48	9.4 ± 4.5	0.848 ± 0.044	0.54 ± 0.07	1.6 ± 1.1
2952	1261 ± 121	10.6 ± 4.0	1.049 ± 0.045	0.79 ± 0.05	0.9 ± 0.5
2953	308 ± 29	5.0 ± 3.2	1.091 ± 0.133	0.64 ± 0.04	1.6 ± 1.2
2954	2646 ± 246	8.5 ± 3.6	0.953 ± 0.024	0.73 ± 0.03	0.6 ± 0.2
2955	1359 ± 117	7.8 ± 3.3	0.974 ± 0.074	0.68 ± 0.04	1.9 ± 0.4
2956	1683 ± 158	19.9 ± 5.0	0.962 ± 0.046	0.58 ± 0.03	-0.1 ± 0.3
2957	423 ± 41	7.0 ± 3.6	1.215 ± 0.127	0.61 ± 0.10	2.8 ± 1.4
2958	418 ± 48	3.6 ± 3.7	1.142 ± 0.120	0.37 ± 0.09	1.3 ± 1.5
2971	308 ± 37	-3.5 ± 3.0	1.449 ± 0.244	0.02 ± 0.07	8.2 ± 7.9

Table 3.4: SAR quality parameters

For each sample, the mean, weighted mean and a robust mean were calculated, as given in Table 3.5. The dose distributions for each sample (Appendix A) all show a broad range of doses, with either a single broad peak or several different peaks, with in many cases a tail to higher dose. In all cases, the weighted mean corresponds more closely to the centre of the major peak than either the mean or robust mean, which are larger in all cases. The weighted mean has, therefore, been selected as the most appropriate estimate of the stored dose, with the exceptions of sample SUTL2952, where this was biased by two aliquots with very low stored dose estimates and the mean was used, and SUTL2958 where all estimates agreed and the mean had the lower uncertainty.

The calculated ages for these samples are given in Table 3.6, combined the preferred stored dose estimate (Table 3.5) with the total dose rate (Table 3.3).

SUTL no.	Comments on stored dose distribution / individual samples	Mean	Weighted Mean	Robust Mean
2941	Peaks in distribution at ~1.0 and ~2.0 Gy, with tail to ~6 Gy	1.82 ± 0.21	**1.29 ± 0.08**	1.74 ± 0.04
2942	Peak at ~2 Gy, with shoulder at ~4 Gy and tail to 10 Gy	2.75 ± 0.37	**1.95 ± 0.17**	2.51 ± 0.02
2943	Peak at ~2.5 Gy, tail to 10 Gy	2.89 ± 0.22	**2.51 ± 0.22**	2.89 ± 0.30
2944	Broad distribution, outlier at 20 ± 11 Gy	5.86 ± 1.37	**2.77 ± 0.32**	4.75 ± 1.64
2945	Peaks at ~2.5 Gy and ~5 Gy, tail >20 Gy.	11.65 ± 2.57	**3.39 ± 0.27**	10.84 ± 2.40
2946	Broad distribution 4-9 Gy, tail to >20 Gy	9.17 ± 1.19	**6.32 ± 0.53**	8.22 ± 0.83
2947	Peak at ~6 Gy, second peak at 8-9 Gy, tail to 15 Gy	7.28 ± 0.55	**6.08 ± 0.32**	7.26 ± 0.03
2948	Peak at 4-8 Gy, tail to 15 Gy	6.05 ± 0.46	**5.06 ± 0.15**	5.87 ± 0.40
2949	Peaks at ~0.6 Gy and 1.5-2.0 Gy, tail to 3.5 Gy	1.36 ± 0.10	**0.49 ± 0.13**	1.40 ± 0.04
2950	Broad peak at ~8 Gy, tail to >20 Gy	10.77 ± 1.23	**6.83 ± 0.38**	9.49 ± 0.64
2951	Two peaks at ~3 Gy and ~5 Gy, tail to 20 Gy	7.44 ± 1.54	**4.03 ± 0.36**	6.26 ± 0.09
2952	Peak at ~1.1 Gy, two aliquots <0.5 Gy	**1.27 ± 0.14**	0.41 ± 0.05	1.32 ± 0.01
2953	Peak at ~1.2 Gy, shoulder at ~2.5 Gy, tail to 10 Gy	2.56 ± 0.33	**1.45 ± 0.15**	2.05 ± 0.09
2954	Peaks at ~3 Gy and ~5 Gy, outlier at 16 ± 4 Gy	4.60 ± 0.80	**3.16 ± 0.17**	3.99 ± 0.11
2955	Peak at ~3 Gy, tail to 10 Gy	3.44 ± 0.26	**2.73 ± 0.21**	3.44 ± 0.30
2956	Peaks at ~4 Gy and ~8 Gy	8.14 ± 1.07	**5.59 ± 0.27**	7.51 ± 0.12
2957	Peak at ~1 Gy, tail to 10 Gy	2.37 ± 0.49	**1.13 ± 0.10**	2.06 ± 0.31
2958	Broad peak at ~5 Gy. Linear dose response curve used	**5.30 ± 0.19**	5.32 ± 1.14	5.43 ± 0.21
2971	Broad peak at ~0.8 Gy with tail to 4 Gy.	3.48 ± 1.69	**0.83 ± 0.14**	1.20 ± 0.19

Table 3.5: Comments on equivalent dose distributions; preferred estimates in bold

errors stated: ± weighted standard deviation (weighted error)

SUTL no.	Transect	Dose (Gy)	Dose Rate (mGy a^{-1})	Years / ka	Calendar years
2941	A (Santa Cruz)	1.29 ± 0.08	3.01 ± 0.14	0.429 ± 0.033	1588 ± 33 AD
2942		1.95 ± 0.17	3.35 ± 0.15	0.582 ± 0.057	1435 ± 57 AD
2943		2.51 ± 0.22	2.97 ± 0.13	0.845 ± 0.083	1172 ± 83 AD
2944		2.77 ± 0.32	3.10 ± 0.14	0.894 ± 0.111	1123 ± 111 AD
2945		3.39 ± 0.27	2.24 ± 0.09	1.513 ± 0.135	504 ± 135 AD
2946		6.32 ± 0.53	3.30 ± 0.15	1.915 ± 0.183	102 ± 183 AD
2947		6.08 ± 0.32	2.90 ± 0.12	2.097 ± 0.14	80 ± 140 BC
2948		5.06 ± 0.15	3.14 ± 0.17	1.611 ± 0.099	406 ± 99 AD
2949	B (Novillero)	0.49 ± 0.13	3.52 ± 0.18	0.139 ± 0.038	1878 ± 38 AD
2950		6.83 ± 0.38	2.81 ± 0.15	2.431 ± 0.187	414 ± 187 BC
2951		4.03 ± 0.36	3.42 ± 0.14	1.178 ± 0.116	839 ± 116 AD
2952	C (Toro Mocho)	1.27 ± 0.14	2.67 ± 0.12	0.476 ± 0.057	1541 ± 57 AD
2953		1.45 ± 0.15	3.47 ± 0.17	0.418 ± 0.048	1599 ± 48 AD
2954		3.16 ± 0.17	3.67 ± 0.17	0.861 ± 0.061	1156 ± 61 AD
2955		2.73 ± 0.21	2.85 ± 0.13	0.958 ± 0.086	1059 ± 86 AD
2956		5.59 ± 0.27	3.17 ± 0.14	1.763 ± 0.115	254 ± 115 AD
2957	San Pedro	1.13 ± 0.10	3.49 ± 0.15	0.324 ± 0.032	1693 ± 32 AD
2971		0.83 ± 0.14	3.32 ± 0.12	0.250 ± 0.043	1767 ± 43 AD
2958		5.30 ± 0.19	3.22 ± 0.13	1.646 ± 0.089	371 ± 89 AD

Table 3.6: Quartz OSL ages

4. Discussion and conclusions

Optically Stimulated Luminescence (OSL) measurements have been conducted on quartz grains separated from samples collected from three transects through dune systems at Nayarit, Mexico, along with two river sediment samples. Combined with dose rate measurements on these samples, this has allowed the calculation of dates for each of these samples, and the establishment of a chronology for the strand plain covering approximately 2000 years.

The three transects all show a similar pattern, with dates for the samples collected near the current coast of 1500-1900AD, with samples further from the coast being progressively older, with a span of approximately 2000 years along the transects. For transect A, the final sample (SUTL2948) is an exception to this sequence, being significantly older than both of the next two samples closer to the coast (SUTL2946 and 2947). For transect B, the middle sample (SUTL2950) is significantly older than the samples on either side (SUTL2949 and 2951). For both transects A and C there is a noticeable step in the ages between the 4^{th} and 5^{th} samples of each transect, 619 ± 175 years between SUTL2944 and 2945 (transect A) and 805 ± 144 years between SUTL2955 and 2956 (transect C).

The dates for the upper samples from the San Pedro River (SUTL2957, 1690 ± 30 AD; SUTL2971, 1770 ± 40 AD) are consistent within 2σ though inverted, both are consistent with the dates for the most westerly dunes in each of the three transects, and the date for the lower sample (SUTL2958, 370 ± 90 AD) is similar to the samples from the eastern ends of the transects. These data suggest that the San Pedro River deposit sampled spans the period of dune formation, and that the sediments 100-150cm below current surface were deposited over a short period of time.

References

Aitken, M.J., 1983, Dose rate data in SI units: PACT, v. 9, p. 69–76.
Mejdahl, V., 1979, Thermoluminescence dating: Beta-dose attenuation in quartz grains Archaeometry, v. 21, p. 61-72.
Mejdahl, V., 1983, Feldspar inclusion dating of ceramics and burnt stones, PACT, v. 9, p. 351-364.
NEA, 2000, The JEF-2.2 Nuclear Data Library: Nuclear Energy Agency, Organisation for economic Co-operation and Development. JEFF Report, v. 17.
Prescott, J.R., and Hutton, J.T., 1994, Cosmic ray contributions to dose rates for luminescence and ESR dating: Large depths and long-term time variations: Radiation Measurements, v. 23, p. 497-500.
Sanderson, D.C.W., 1987, Thermoluminescence dating of vitrified Scottish Forts: Paisley, Paisley college.
—, 1988, Thick source beta counting (TSBC): A rapid method for measuring beta dose-rates: International Journal of Radiation Applications and Instrumentation. Part D. Nuclear Tracks and Radiation Measurements, v. 14, p. 203-207.

Acknowledgements

This work was supported by grant DGAPA-PAPIIT(UNAM) IN105517.

Appendix A: Dose Response Curves and Probability Distributions

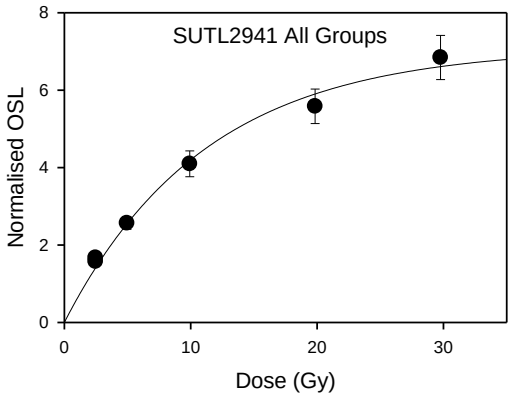

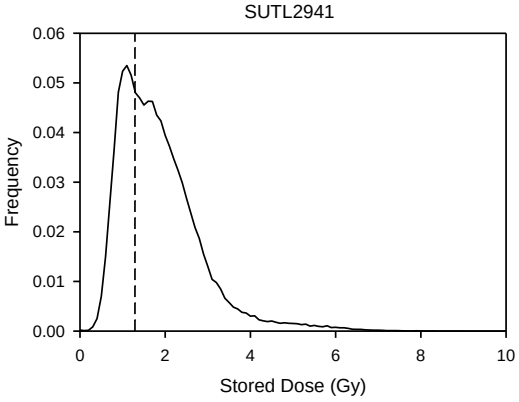

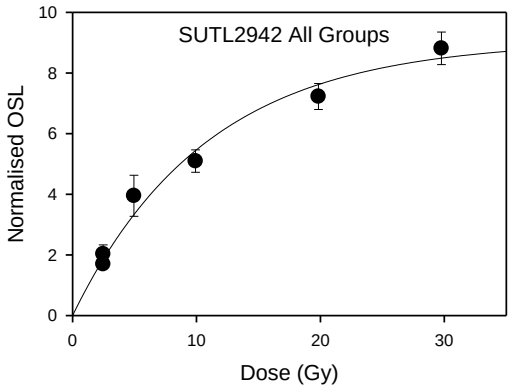

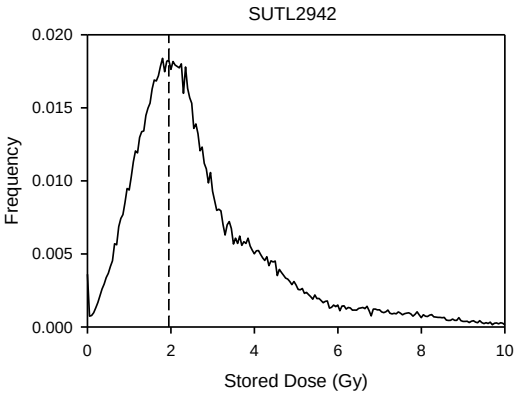

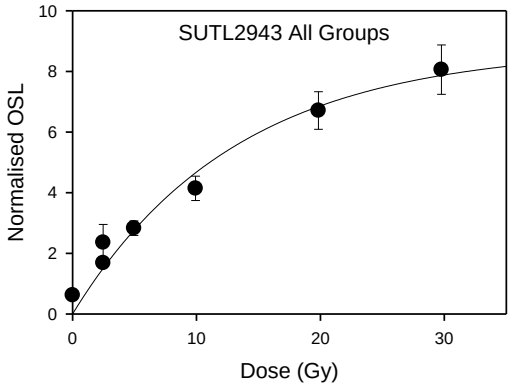

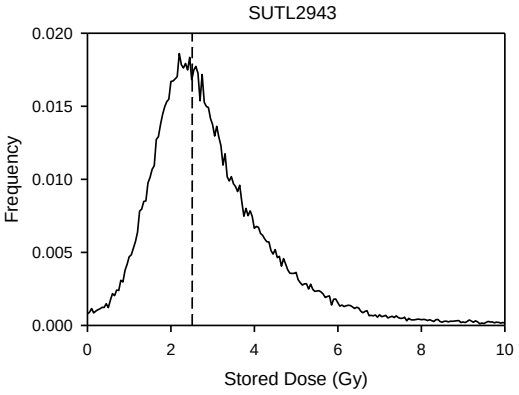

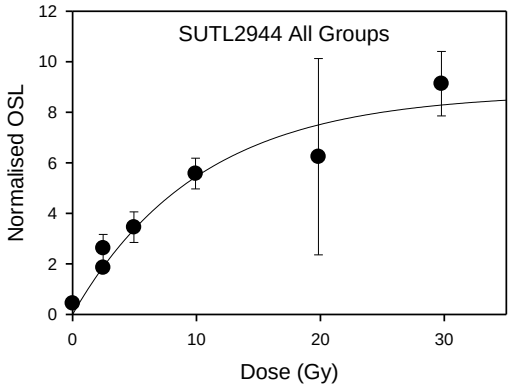

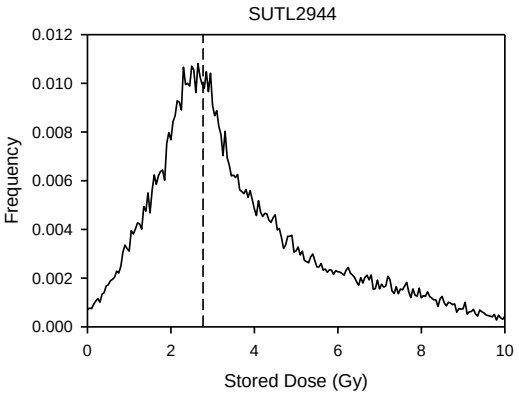

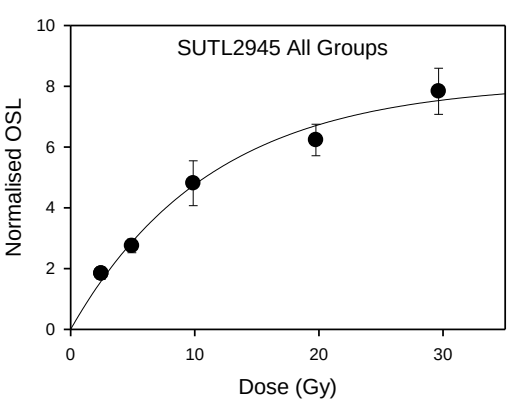
SUTL2945 All Groups
Normalised OSL
Dose (Gy)

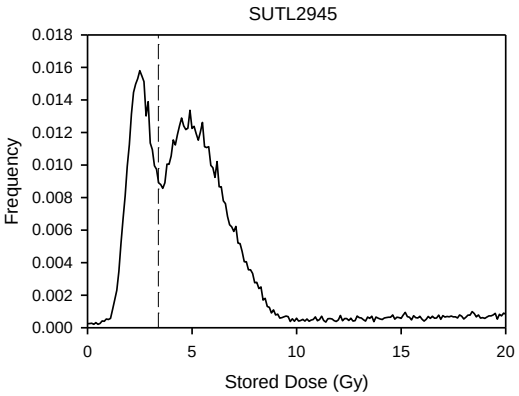
SUTL2945
Frequency
Stored Dose (Gy)

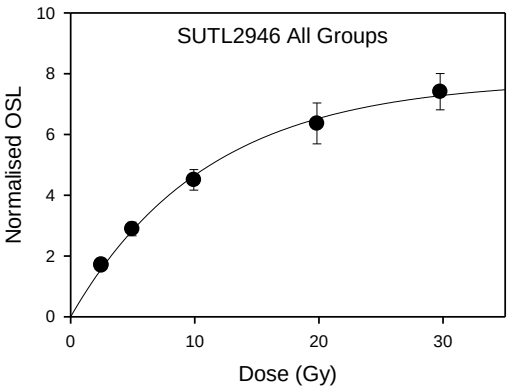
SUTL2946 All Groups
Normalised OSL
Dose (Gy)

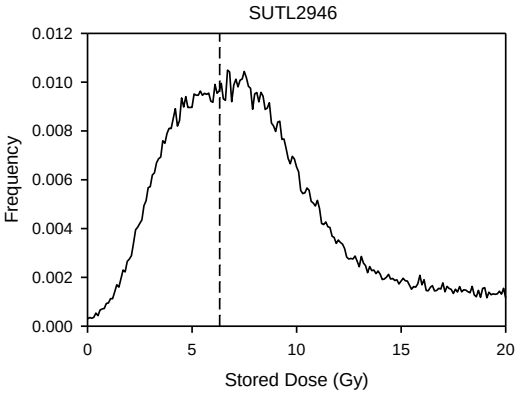
SUTL2946
Frequency
Stored Dose (Gy)

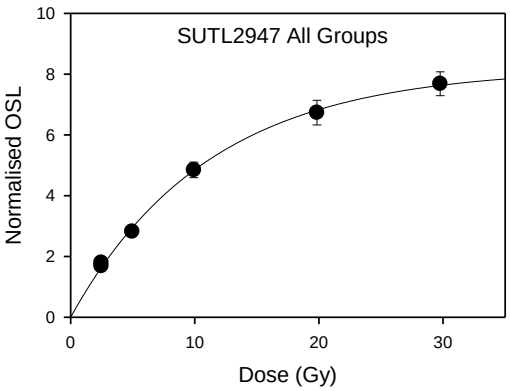
SUTL2947 All Groups
Normalised OSL
Dose (Gy)

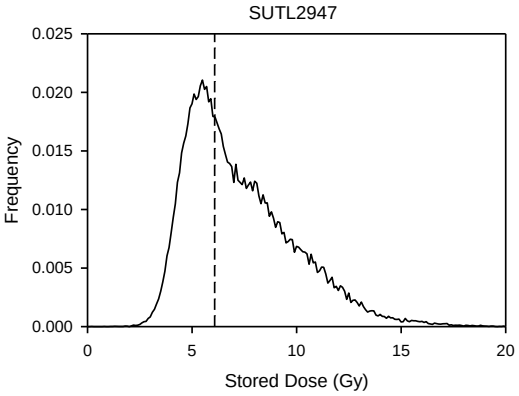
SUTL2947
Frequency
Stored Dose (Gy)

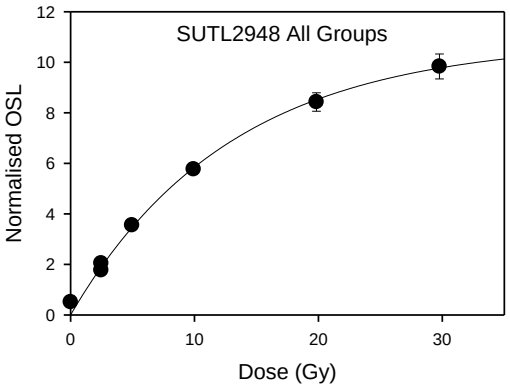
SUTL2948 All Groups
Normalised OSL
Dose (Gy)

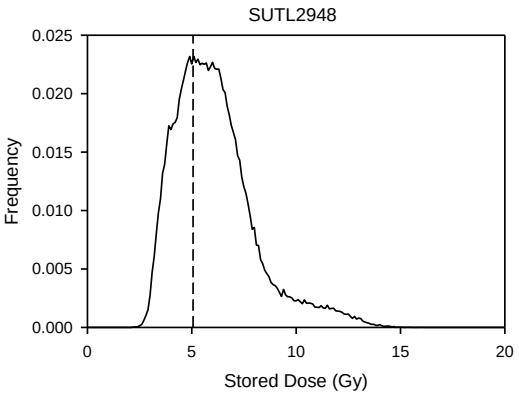
SUTL2948
Frequency
Stored Dose (Gy)

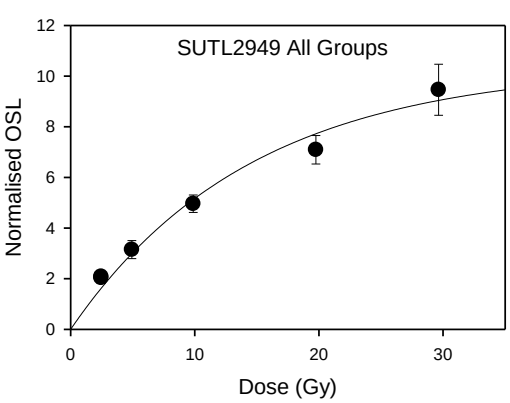
SUTL2949 All Groups
Normalised OSL
Dose (Gy)

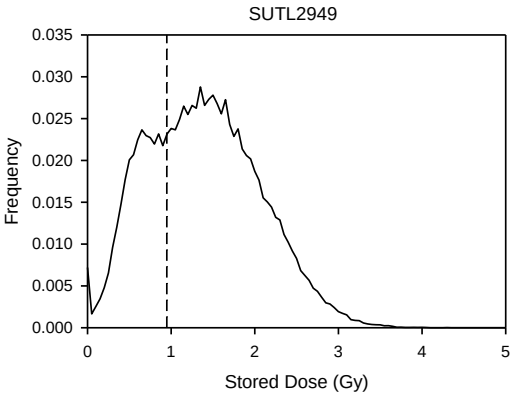
SUTL2949
Frequency
Stored Dose (Gy)

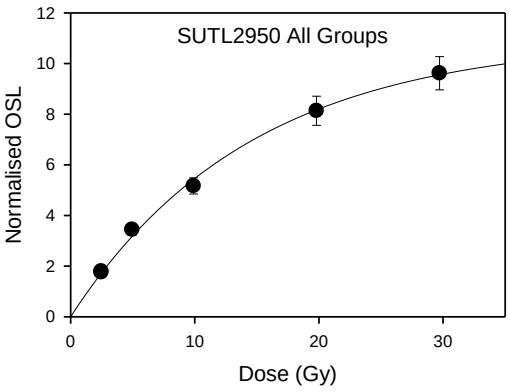
SUTL2950 All Groups
Normalised OSL
Dose (Gy)

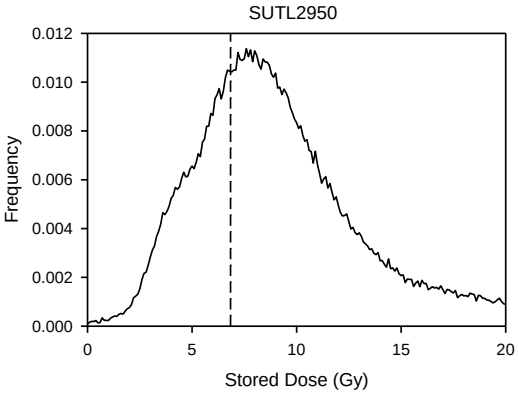
SUTL2950
Frequency
Stored Dose (Gy)

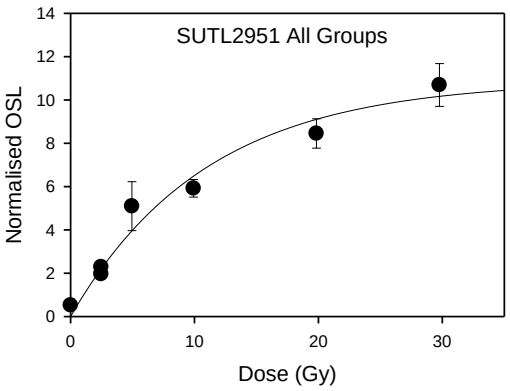
SUTL2951 All Groups
Normalised OSL
Dose (Gy)

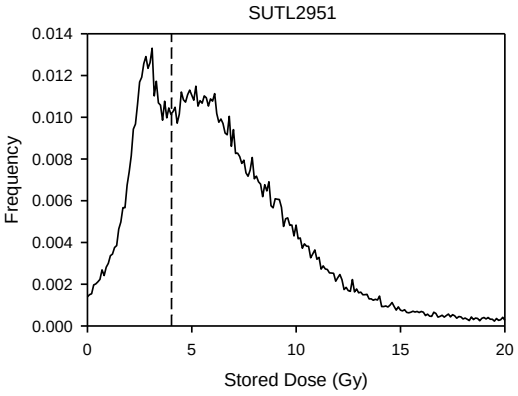
SUTL2951
Frequency
Stored Dose (Gy)

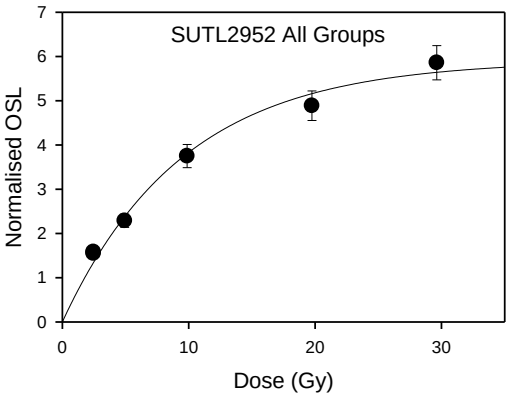
SUTL2952 All Groups
Normalised OSL
Dose (Gy)

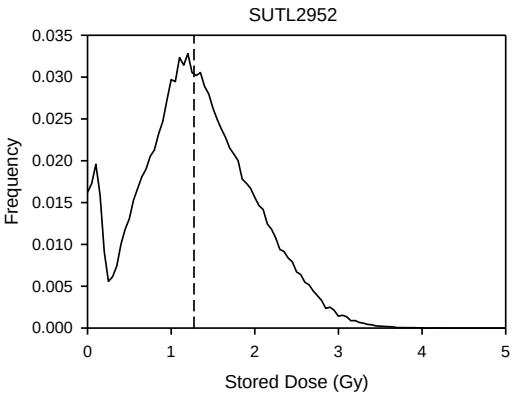
SUTL2952
Frequency
Stored Dose (Gy)

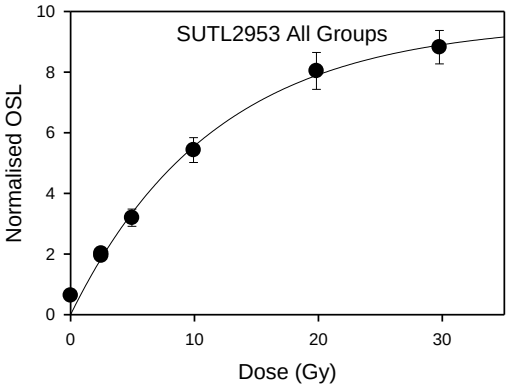
SUTL2953 All Groups
Normalised OSL
Dose (Gy)

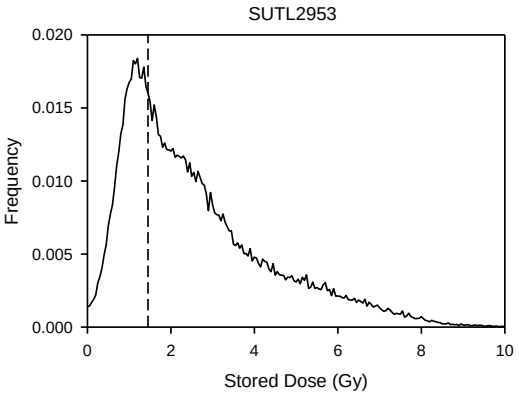
SUTL2953
Frequency
Stored Dose (Gy)

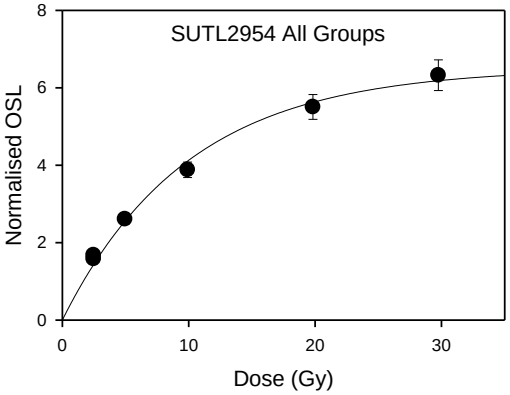
SUTL2954 All Groups
Normalised OSL
Dose (Gy)

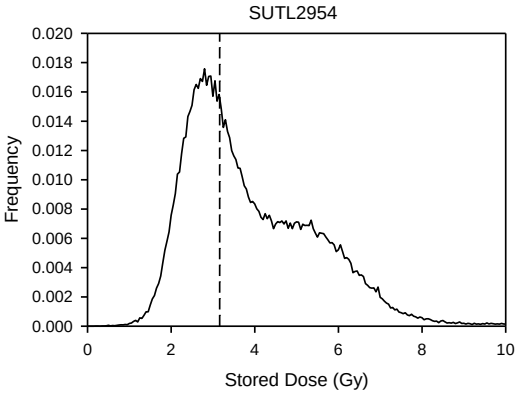
SUTL2954
Frequency
Stored Dose (Gy)

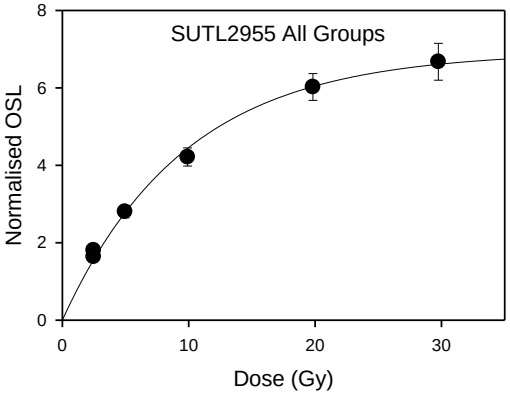
SUTL2955 All Groups
Normalised OSL
Dose (Gy)

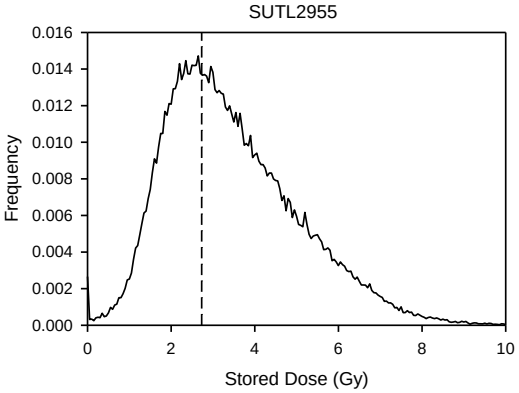
SUTL2955
Frequency
Stored Dose (Gy)

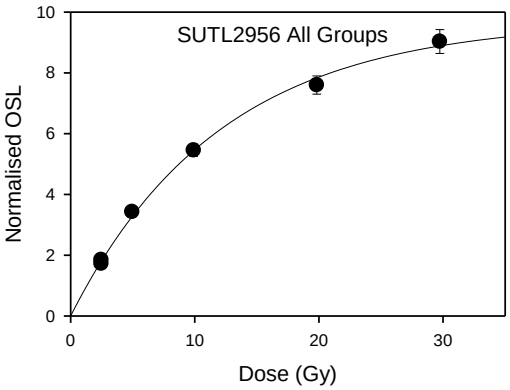
SUTL2956 All Groups
Normalised OSL
Dose (Gy)

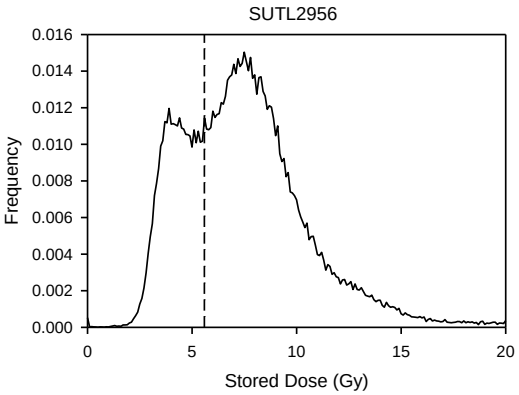
SUTL2956
Frequency
Stored Dose (Gy)

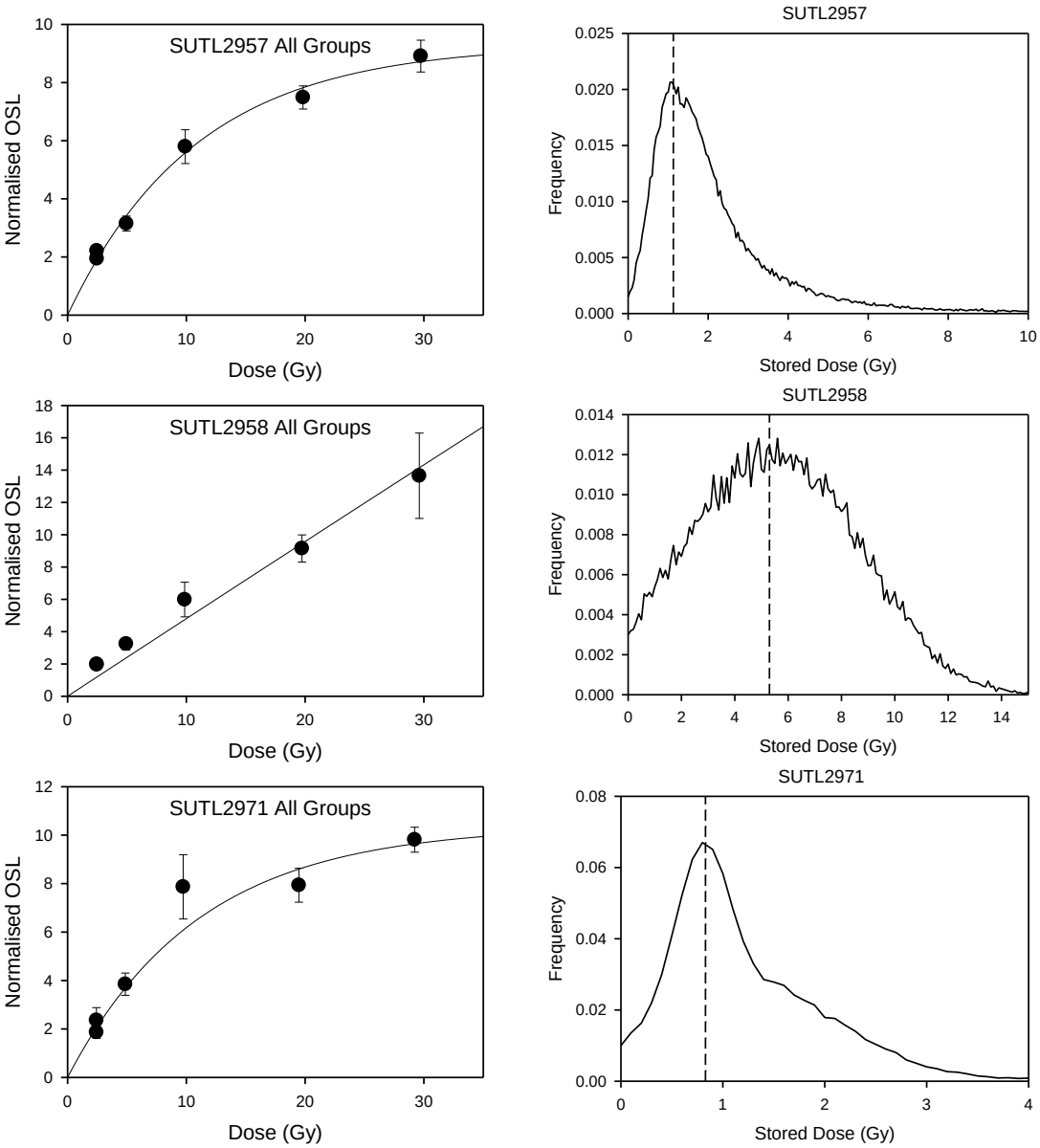
SUTL2957 All Groups
Normalised OSL
Dose (Gy)
SUTL2957
Frequency
Stored Dose (Gy)
SUTL2958 All Groups
Normalised OSL
Dose (Gy)
SUTL2958
Frequency
Stored Dose (Gy)
SUTL2971 All Groups
Normalised OSL
Dose (Gy)
SUTL2971
Frequency
Stored Dose (Gy)

Appendix B: Abanico Plots

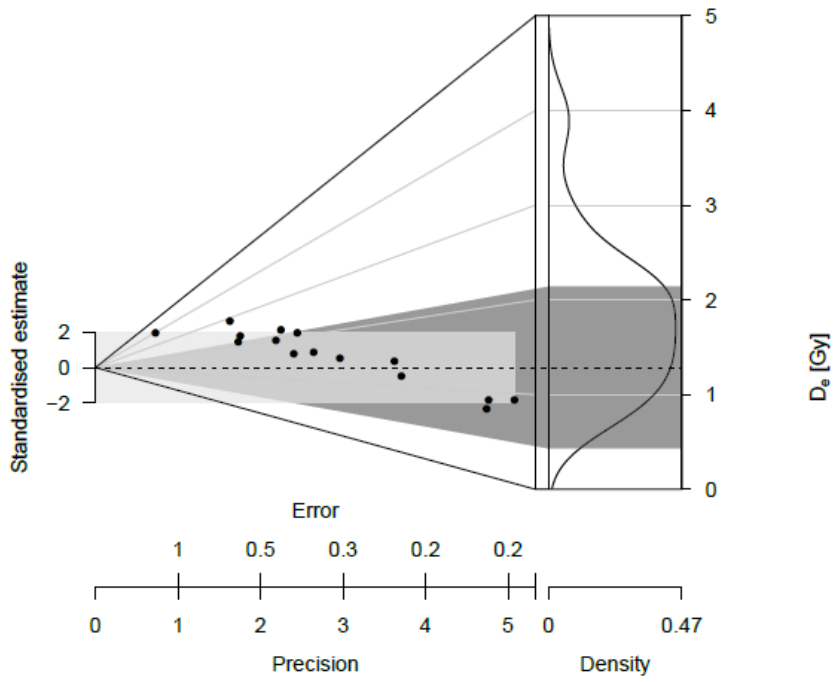

Figure B.1: Abanico Plot for SUTL2941. The dashed line indicates the weighted mean.

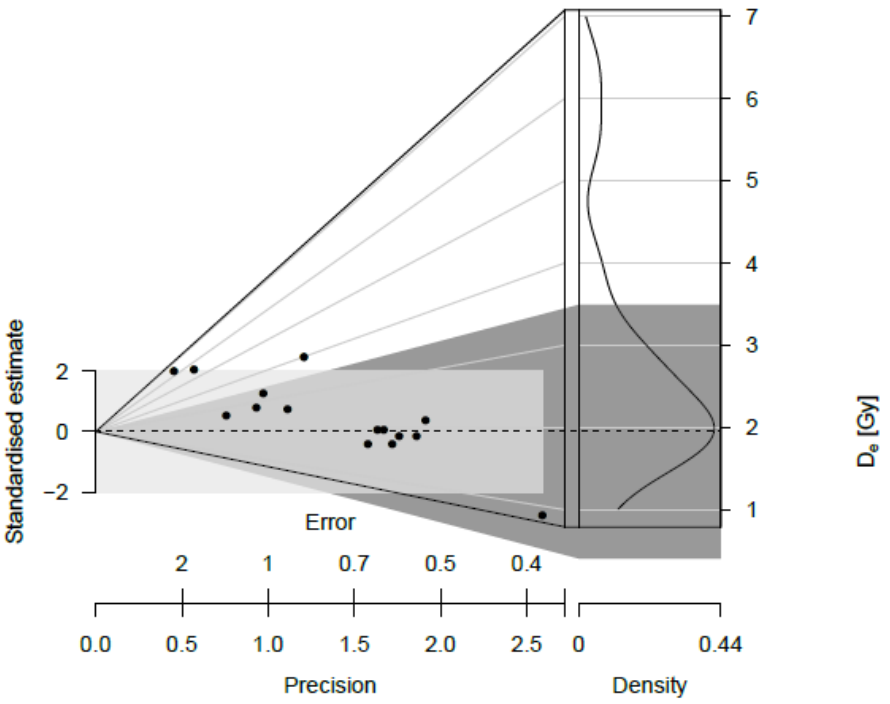

Figure B.2: Abanico Plot for SUTL2942. The dashed line indicates the weighted mean.

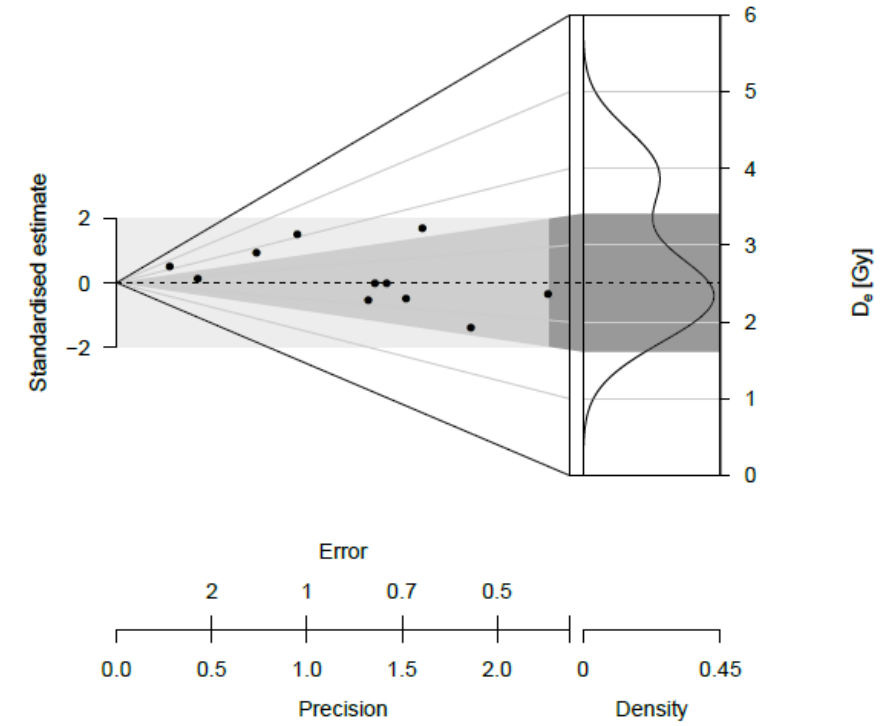

Figure B.3: Abanico Plot for SUTL2943. The dashed line indicates the weighted mean.

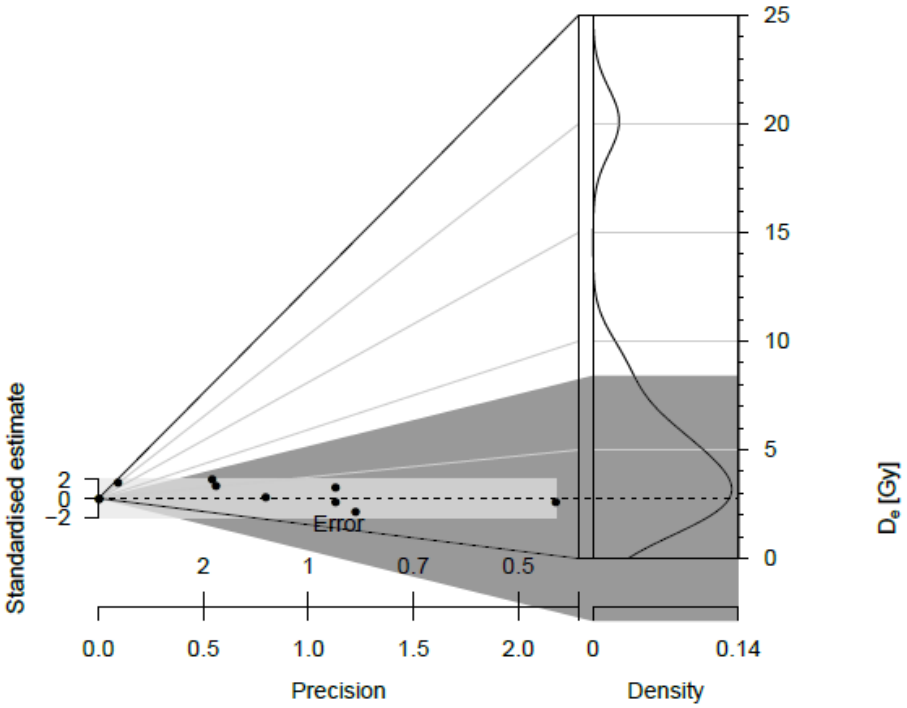

Figure B.4: Abanico Plot for SUTL2944. The dashed line indicates the weighted mean.

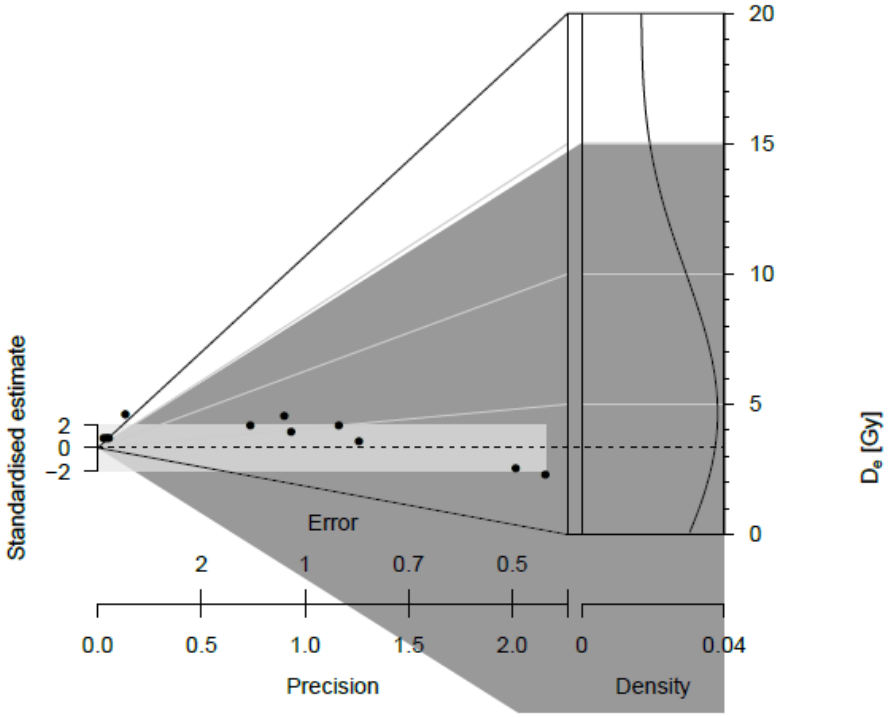

Figure B.5: Abanico Plot for SUTL2945. The dashed line indicates the weighted mean.

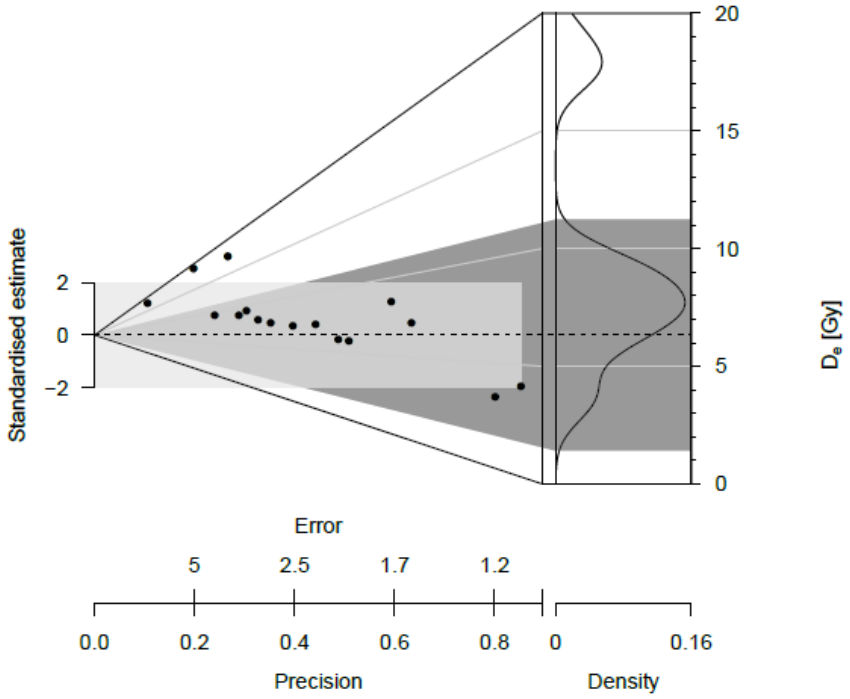

Figure B.6: Abanico Plot for SUTL2946. The dashed line indicates the weighted mean.

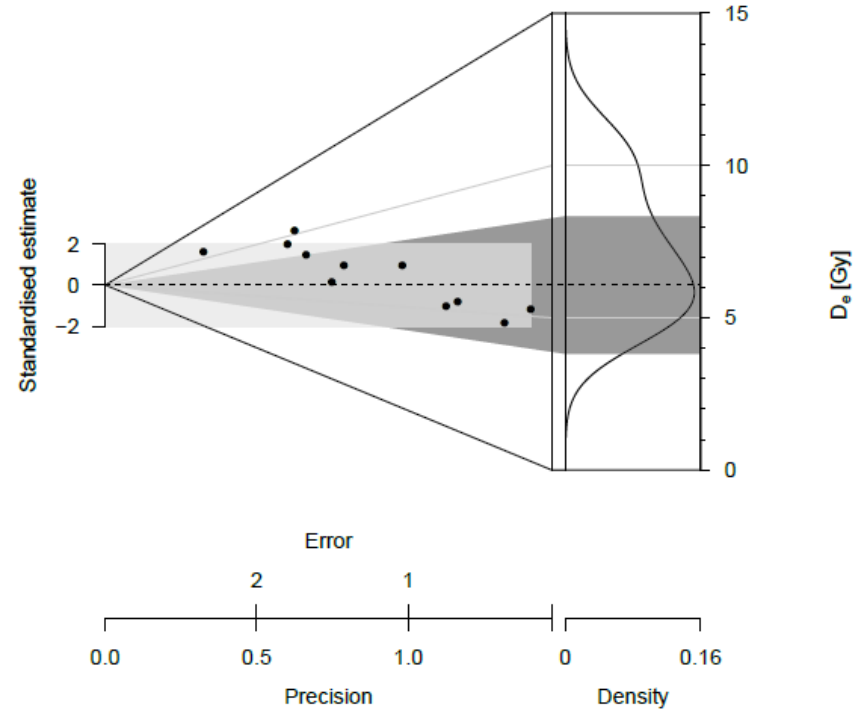

Figure B.7: Abanico Plot for SUTL2947. The dashed line indicates the weighted mean.

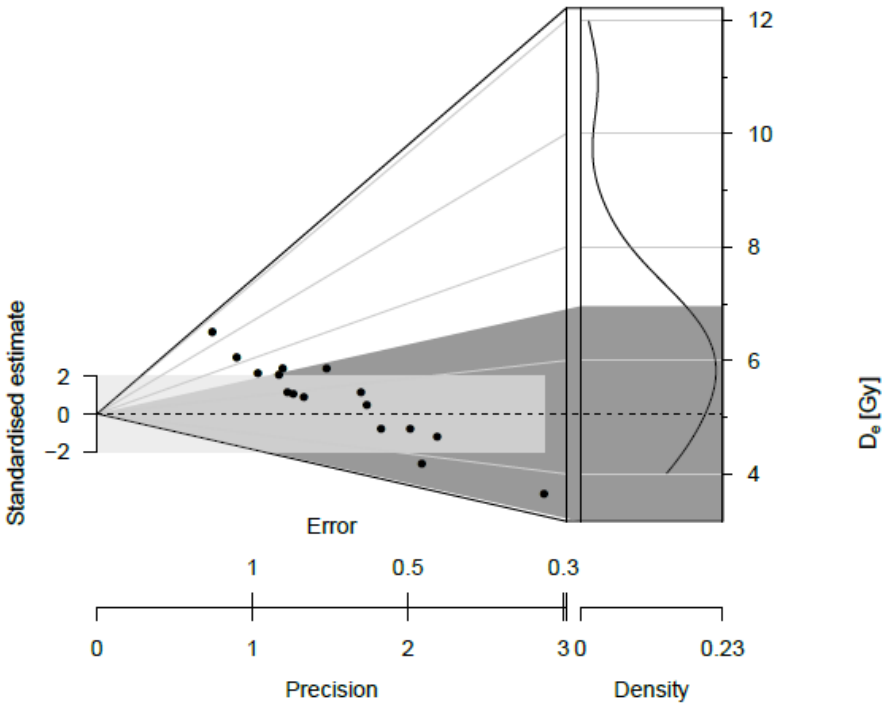

Figure B.8: Abanico Plot for SUTL2948. The dashed line indicates the weighted mean.

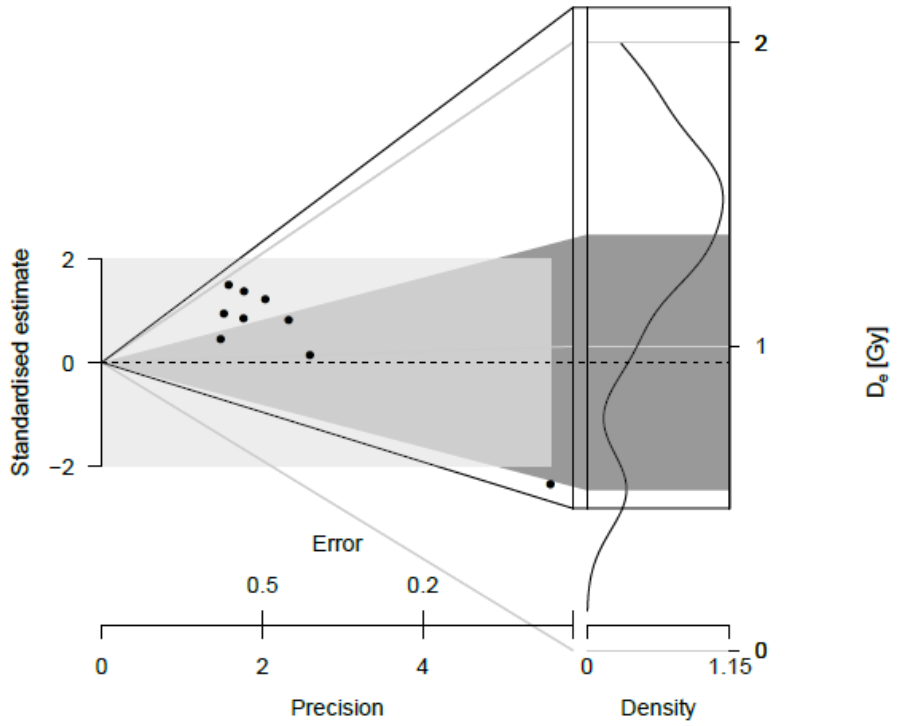

Figure B.9: Abanico Plot for SUTL2949. The dashed line indicates the weighted mean.

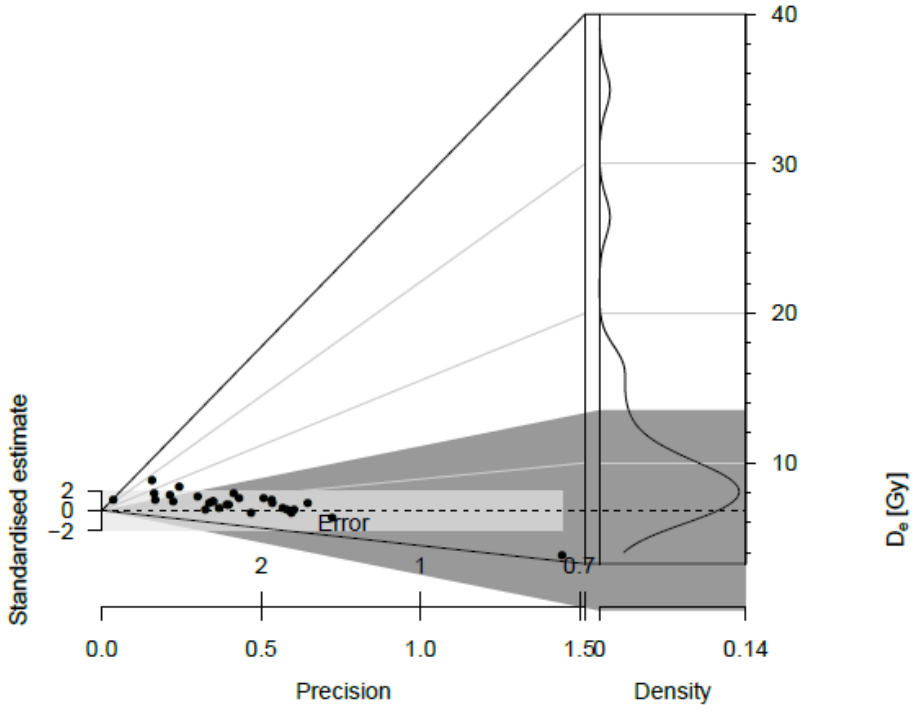

Figure B.10: Abanico Plot for SUTL2950. The dashed line indicates the weighted mean.

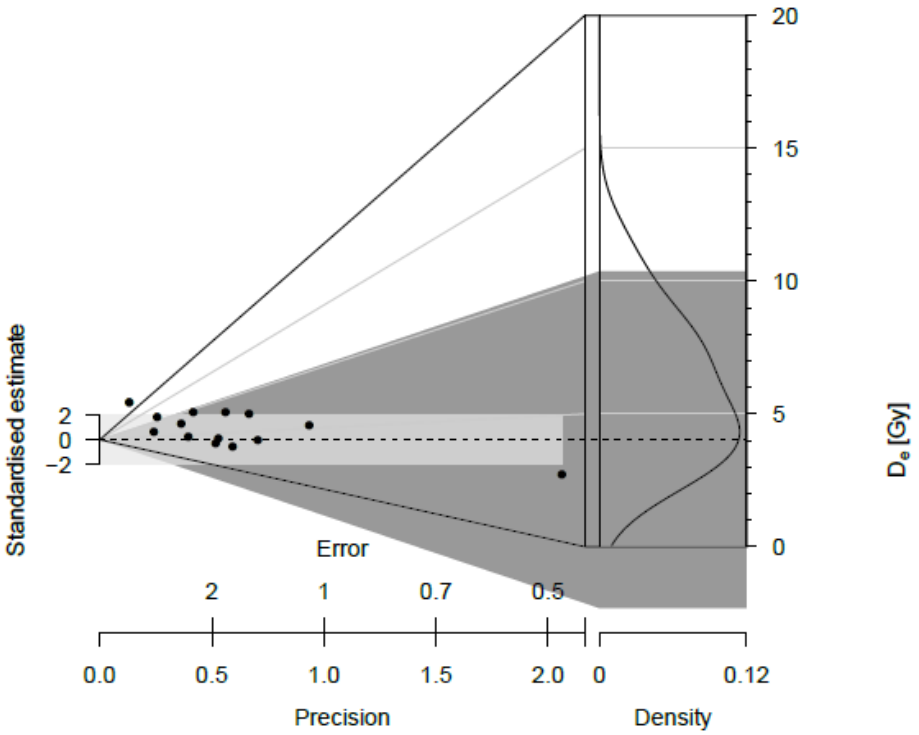

Figure B.11: Abanico Plot for SUTL2951. The dashed line indicates the weighted mean.

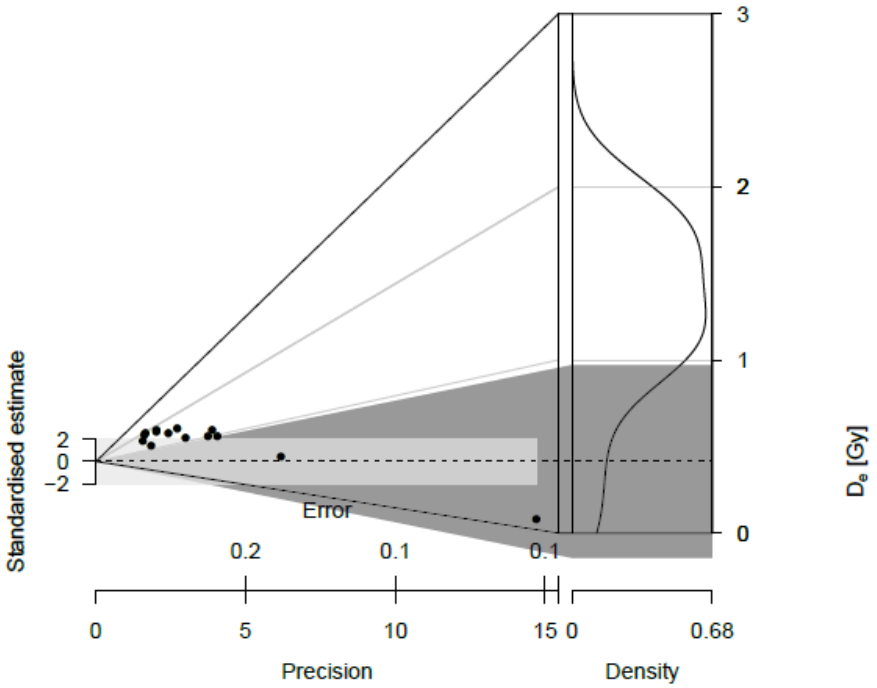

Figure B.12: Abanico Plot for SUTL2952. The dashed line indicates the weighted mean.

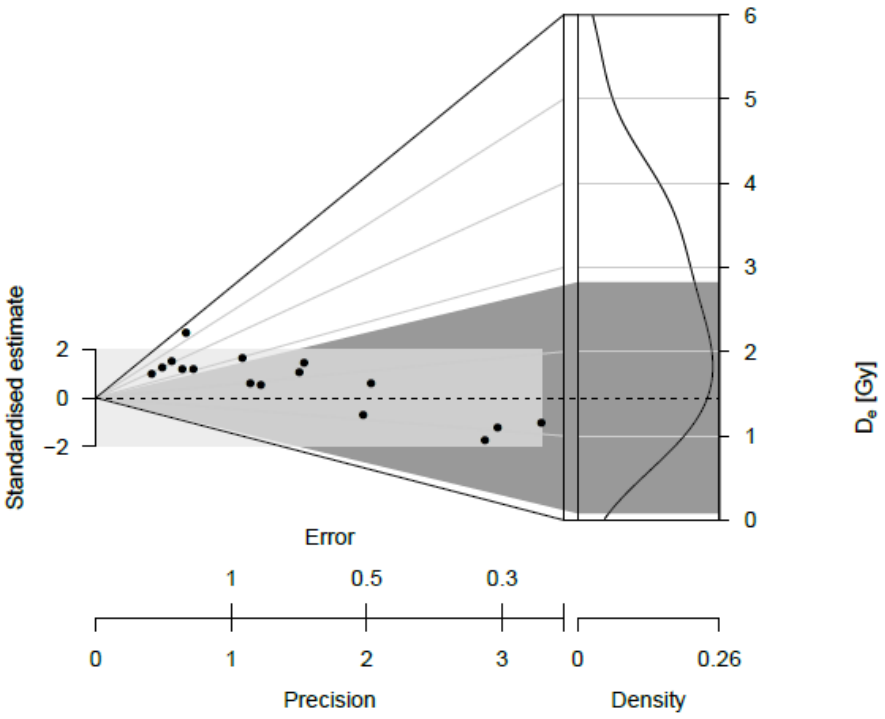

Figure B.13: Abanico Plot for SUTL2953. The dashed line indicates the weighted mean.

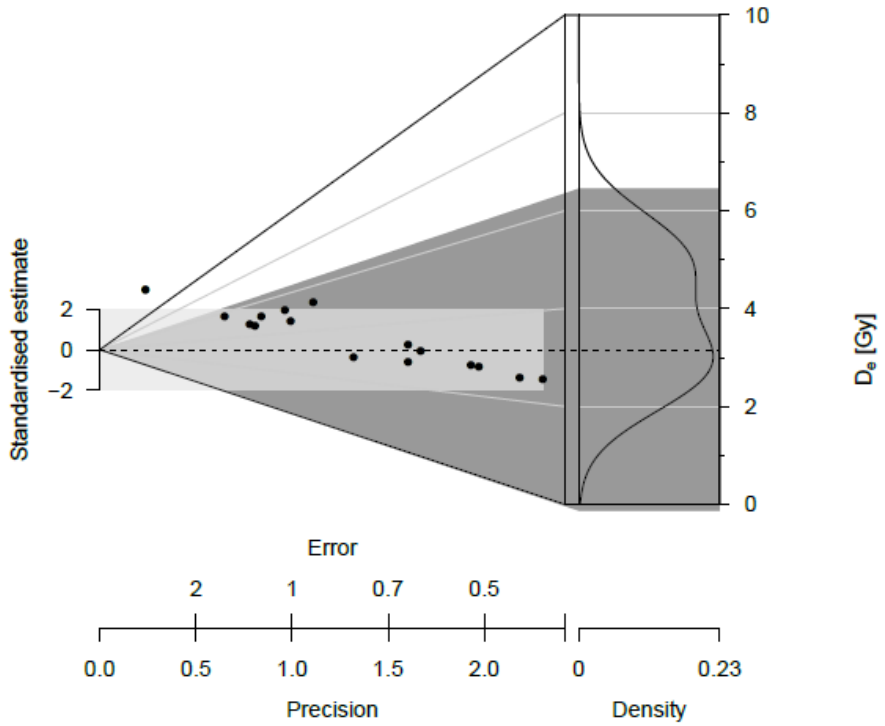

Figure B.14: Abanico Plot for SUTL2954. The dashed line indicates the weighted mean.

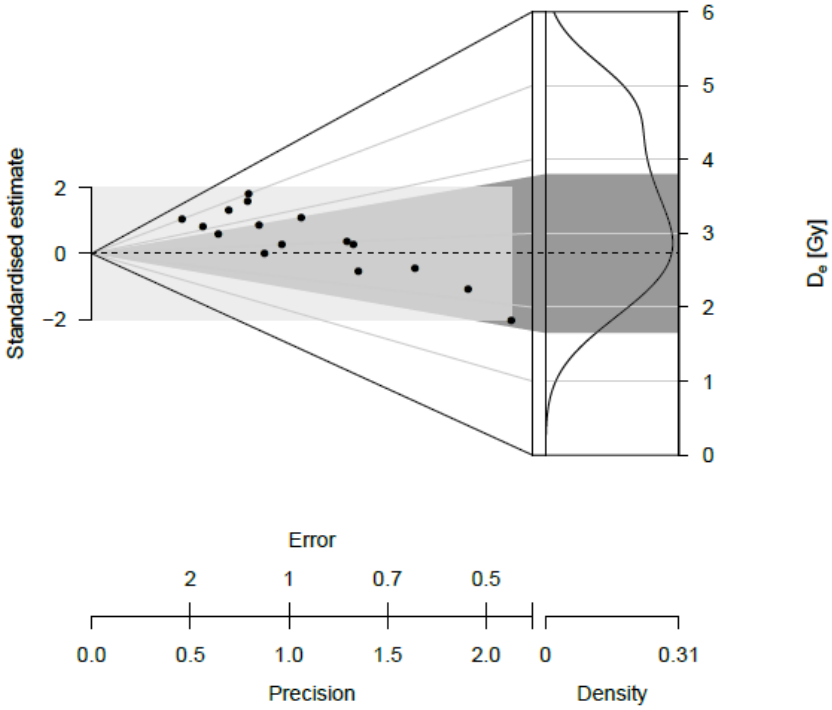

Figure B.15: Abanico Plot for SUTL2955. The dashed line indicates the weighted mean.

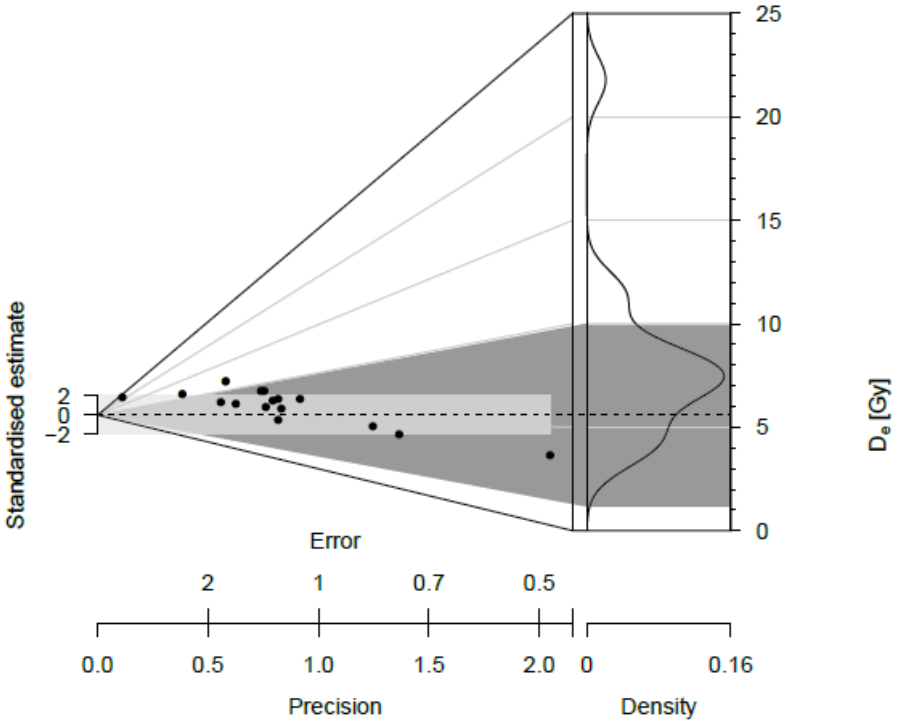

Figure B.16: Abanico Plot for SUTL2956. The dashed line indicates the weighted mean.

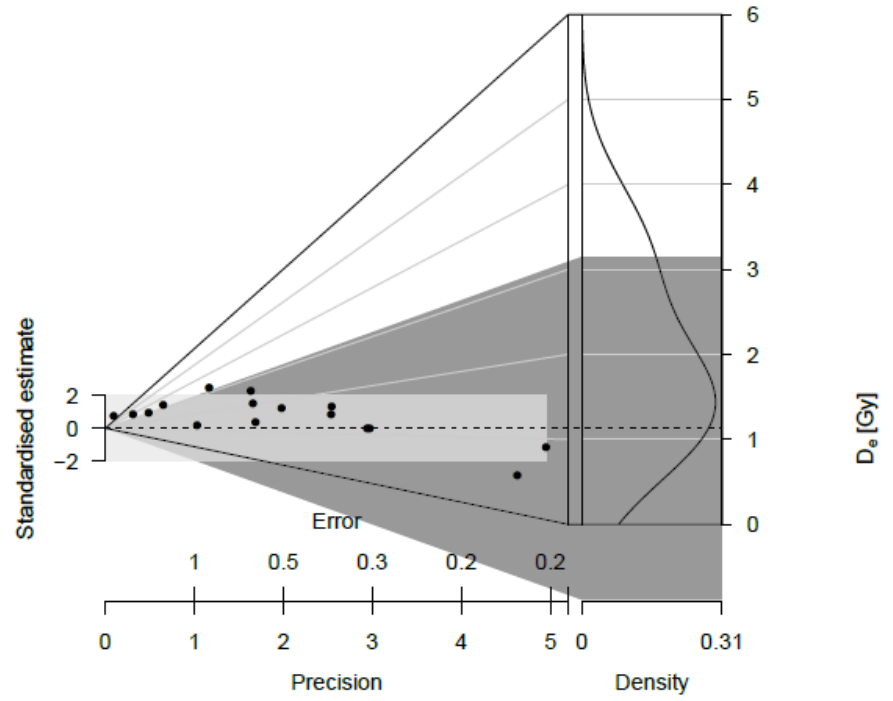

Figure B.17: Abanico Plot for SUTL2957. The dashed line indicates the weighted mean.

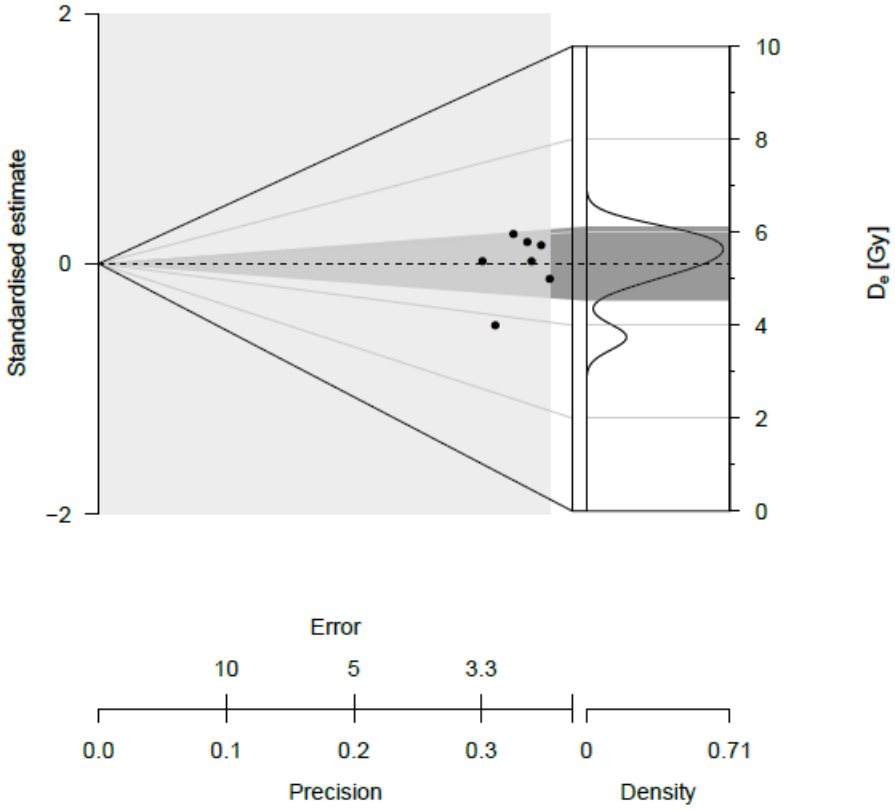

Figure B.18: Abanico Plot for SUTL2958. The dashed line indicates the weighted mean.

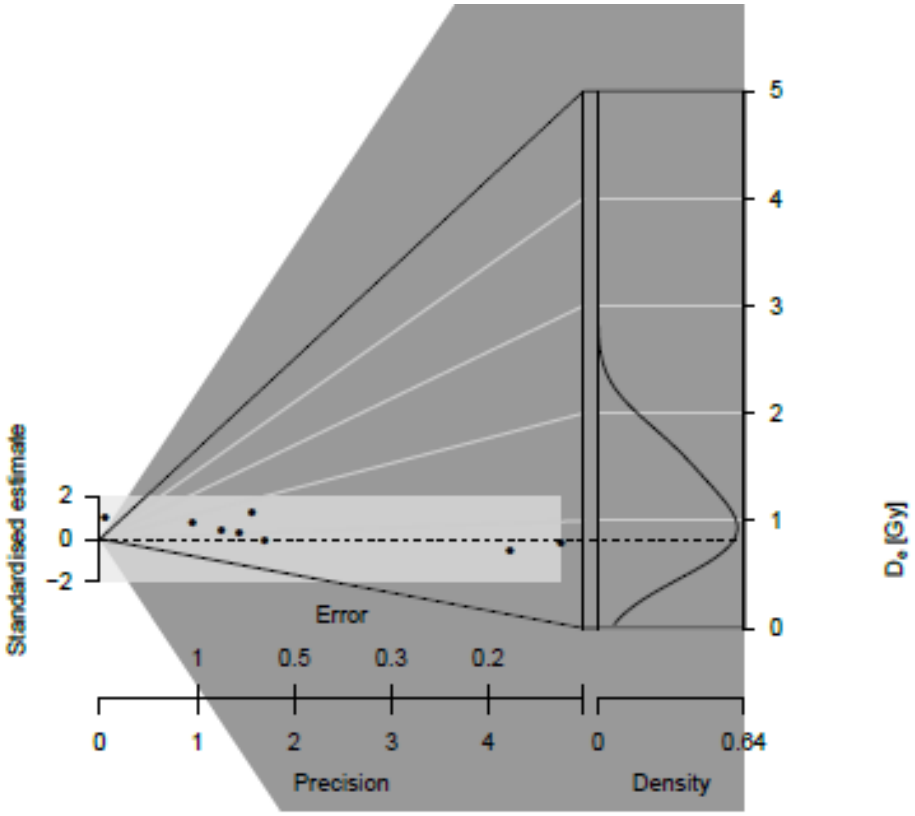

Figure B.19: Abanico Plot for SUTL2971. The dashed line indicates the weighted mean. The plot excludes an aliquot at 20 Gy.